



## *Calanus finmarchicus* seasonal cycle and diapause in relation to gene expression, physiology, and endogenous clocks

N. Sören Häfker <sup>1,2\*</sup> M. Teschke,<sup>1</sup> K. S. Last,<sup>3</sup> D. W. Pond,<sup>3</sup> L. Hüppe,<sup>2</sup> B. Meyer <sup>1,2,4\*</sup>

<sup>1</sup>Alfred Wegener Institute Helmholtz Centre for Polar and Marine Research, Bremerhaven, Germany

<sup>2</sup>Institute for Chemistry and Biology of the Marine Environment, University of Oldenburg, Oldenburg, Germany

<sup>3</sup>Scottish Association for Marine Science, Oban, Argyll, UK

<sup>4</sup>Helmholtz Institute for Functional Marine Biodiversity at the University of Oldenburg, Oldenburg, Germany

### Abstract

The copepod *Calanus finmarchicus* plays a crucial role in the north Atlantic food web. Its seasonal life cycle involves reproduction and development in surface waters before overwintering in diapause at depth. Although diapause has been studied for more than a century, the factors responsible for the initiation and termination of it are still unclear. Endogenous clocks have been identified as potent tools for photoperiod measurement and seasonal rhythmicity in many terrestrial species, but knowledge of these remains scarce in the marine realm. Focusing on the dominant CV copepodid stage, we sampled a population of *C. finmarchicus* from a Scottish sea loch to characterize population dynamics, several physiological parameters, and diel and seasonal expression rhythms of 35 genes representing different metabolic pathways, including the circadian clock machinery. This generated a detailed overview of the seasonal cycle of *C. finmarchicus* including the most extensive field dataset on circadian clock gene expression in a marine species to date. Gene expression patterns revealed distinct gene clusters upregulated at different phases of the copepod's seasonal cycle. While diel clock cycling was restricted to the active spring/summer phase, many clock genes exhibited the highest expression during diapause. Our results provide new insights into diapause on physiological and genetic levels. We suggest that photoperiod, in interaction with internal and external factors (lipid content, temperature, food availability) and the endogenous clock mechanism, plays an important role in the timing of diapause in *C. finmarchicus*.

The calanoid copepod *Calanus finmarchicus* (Gunnerus, 1770) is an ecological key species in the Northern Atlantic (Runge 1988). The species often dominates zooplankton biomass between 40°N and 80°N (Conover 1988; Kwasniewski et al. 2003; Helaouët and Beaugrand 2007). *C. finmarchicus* predominantly feeds on phytoplankton (Marshall and Orr 1955; Harris et al. 2000) and accumulates large lipid reserves for overwintering (Falk-Petersen et al. 2009), making the copepod an important energy source for higher trophic levels including several commercially important fish stocks (Sundby 2000; Prokopchuk and Sentyabov 2006).

The seasonal cycle of *C. finmarchicus* is initiated by adults from the overwintering stock mating and spawning eggs prior to

and during the spring bloom (Niehoff et al. 1999; Harris et al. 2000). The new generation develops through several nauplii (NI–NVI) and juvenile copepodid stages (CI–CV) before again reaching the adult female or male stage (CVIf or CVIm, respectively) (Marshall and Orr 1955). During this time of activity, development and feeding in shallow waters, *C. finmarchicus* performs diel vertical migration (DVM) (e.g., Irigoien et al. 2004). While predator avoidance is considered the ultimate reason for DVM and predator presence can directly affect migration patterns, light is usually considered the most important proximate cue regulating DVM (Irigoien et al. 2004; Brierley 2014). In the CIV and especially the CV copepodid stage the copepods accumulate large amounts of lipids, predominantly wax esters stored in a lipid sac (Falk-Petersen et al. 2009; Clark et al. 2013). From the CV stage on the life cycle can progress in two different ways (Tarrant et al. 2014, 2016). The CVs either migrate into deeper water where they enter a prolonged phase of inactivity commonly referred to as diapause (Hirche 1996a) or they remain in surface waters and continue development, molting into adults to produce a second generation. The second generation then develops until the CV stage prior to again either entering diapause or maturing to produce another generation that enters

\*Correspondence: soeren.haefker@awi.de; bettina.meyer@awi.de

This is an open access article under the terms of the Creative Commons Attribution-NonCommercial-NoDerivs License, which permits use and distribution in any medium, provided the original work is properly cited, the use is non-commercial and no modifications or adaptations are made.

Additional Supporting Information may be found in the online version of this article.

diapause even later (Miller et al. 1991; Johnson et al. 2008). While the number of generations and timing of descent is similar between years for any given population, there are geographic differences (Melle et al. 2014). *C. finmarchicus* in an Arctic fjord produces one generation per year, whereas a population in the Gulf of Maine produces up to three generations (Durbin et al. 2000; Walkusz et al. 2009).

During diapause, the copepods have reduced gut epithelium and show reduced metabolic activity and development (Hallberg and Hirche 1980; Hirche 1996a; Ingvarsdóttir et al. 1999). Diapause depth in the open ocean is usually between 400 m and 1000 m (Hirche 1996a; Heath et al. 2004) but in coastal habitats (lochs and fjords) *C. finmarchicus* has been found to diapause close to the bottom between 100 m and 150 m (Clark et al. 2013). The copepods stay in diapause for several months before increasing metabolic activity and the development of gonadal tissues mark the emergence from diapause (Hirche 1996a,b). This starts in late autumn/early winter well before the copepods molt to adults and mate during their ascent to the surface (usually in February–April) (Marshall and Orr 1955; Hirche 1996a). While the seasonal cycle of *C. finmarchicus* and its congeners has been described in great detail with regard to their population dynamics (e.g., Plourde et al. 2001) and physiology (e.g., Clark et al. 2012; Freese et al. 2015, 2017), seasonal investigations on the genetic level are still rare (Tarrant et al. 2008; Clark et al. 2013) and the processes controlling the timing of the copepods annual life cycle are far from understood (Ji 2011; Baumgartner and Tarrant 2017).

Diapause initiation in *C. finmarchicus* has most prominently been linked to lipid content (Rey-Rassat et al. 2002; Johnson et al. 2008; Tarrant et al. 2008; Pond et al. 2012) with a minimum lipid content required prior to diapause initiation to survive the time without feeding at depth (Saumweber and Durbin 2006; Maps et al. 2011). Alternatively, the presence of predator kairomones was shown to trigger diapause in different zooplankton species (Lass and Spaak 2003) and it has further been proposed that decreasing phytoplankton concentrations trigger the descent to diapause after the spring bloom (Hind et al. 2000; Wilson et al. 2016). The seasonal change of photoperiod (day length) has also been suggested as a possible cue for diapause initiation (Grigg and Bardwell 1982; Miller et al. 1991). However, to date the trigger(s) of diapause remain unresolved (Tarrant et al. 2016; Baumgartner and Tarrant 2017).

While the same population can produce two or more generations which enter diapause at different times of the year (e.g., Johnson et al. 2008), emergence from diapause often occurs over a comparably short time span within a given population with the suggestion that it is “synchronized” (Baumgartner and Tarrant 2017). An “hourglass” timer has been proposed that starts “ticking” with the initiation of diapause and ultimately triggers emergence (Miller et al. 1991; Campbell et al. 2004). This mechanism could be initiated by

decreasing lipid levels, the accumulation of hormones or continuous slow development (Hind et al. 2000; Irigoien 2004; Clark et al. 2012), but it does not account for the synchronized emergence of copepods from generations that entered diapause at different times. Another hypothesis suggests that photoperiod could be a cue for synchronizing emergence from diapause (Miller et al. 1991; Tittensor et al. 2003; Speirs et al. 2005). There have been several model studies simulating *C. finmarchicus* diapause initiation and termination based on the above parameters (for overview see Baumgartner and Tarrant 2017), but it has so far not been possible to generate the seasonal cycle of diapause initiation and termination under controlled laboratory conditions. While the significance of lipid content, food availability, and temperature for *C. finmarchicus* seasonal timing has already received attention (Ingvarsdóttir et al. 1999; Rey-Rassat et al. 2002; Hassett 2006; Saumweber and Durbin 2006; Johnson et al. 2008; Clark et al. 2012; Pierson et al. 2013), research on the effects of photoperiod is still scarce (Miller et al. 1991; Johnson et al. 2008).

Many terrestrial organisms measure photoperiod using a circadian clock to predict cyclic seasonal change (Oster et al. 2002; Meuti and Denlinger 2013). Like countless other organisms *C. finmarchicus* possesses a circadian clock, which consists of “clock genes” that form the core regulatory component of the circadian machinery (Mackey 2007; Häfker et al. 2017). These genes interact via their protein products forming an intricate network of feedback loops that result in an endogenous rhythm of ~ 24-h length (Latin: “*circa dies*”: about a day). Although able to function independently, the clock is entrained on a regular basis by environmental cues, the most common of which is the light/dark cycle (Aschoff 1954). For many insects, the circadian clock is crucial for measuring photoperiod and for entraining their seasonal life cycle (Oster et al. 2002; Meuti and Denlinger 2013). Also, many insects initiate or terminate diapause when surpassing a certain critical photoperiod marking the transition from one seasonal life phase to another (He et al. 2009; Sakamoto et al. 2009; Goto 2013; Salminen et al. 2015). Photoperiodic entrainment of seasonal diapause has also been demonstrated in the eggs and juveniles of marine and freshwater copepods (Einsle 1964; Watson and Smallman 1971; Marcus 1982) and was suggested for *C. finmarchicus* (Grigg and Bardwell 1982; Miller et al. 1991). However, the molecular and physiological processes underpinning photoperiodic time measurement and the pathways by which such timing mechanisms affect the seasonal life cycle and diapause of copepods, remain unexplored.

Here, we characterize the seasonal cycle of *C. finmarchicus*’ dominant life stage (CV) in a Scottish sea loch. Field sampling provided detailed insights into seasonal patterns of vertical migration rhythms, population dynamics, physiological parameters, and gene expression. We present comprehensive data of diel and seasonal clock gene rhythmicity revealing endogenous timing mechanisms of *C. finmarchicus* and suggest that photoperiod and/or a circannual clock may be

involved in the initiation and termination of *C. finmarchicus* diapause.

## Materials and methods

### Study site characteristics

The investigation took place in Loch Etive, a sea loch in western Scotland, UK (56°45'N, 5°18'W). A sill with a depth of ~ 7 m limits the exchange with the open ocean and a second sill (~ 13 m) further divides the loch into an upper and a lower basin (Edwards and Edelsten 1977; Nørgaard-Pedersen et al. 2006). All sampling was conducted in the upper basin at the deepest point of the loch, Bonawe deep (~ 145 m) (Fig. 1). The deeper waters of the upper basin typically cycle from normoxic to hypoxic and due to the sills, overturning of these water masses happens irregularly every ~ 18 months when spring tides in spring/autumn co-occur with low precipitation (Edwards and Edelsten 1977). To monitor the seasonal changes in the hydrography of the loch, a mooring was deployed close to Bonawe deep (145 m depth) equipped with temperature loggers (SBE 56, Sea-Bird Electronics) attached in 10 m intervals. In addition, salinity, temperature, oxygen concentration, fluorescence-based chlorophyll *a* (Chl *a*) concentration, and photosynthetic active radiation (PAR, 400–700 nm) were recorded by a conductivity–temperature–depth (CTD) profiler (SBE 19plus V2 SeaCAT Profiler, Sea-Bird Electronics) equipped with an irradiance sensor (QSP-2300, Biospherical Instruments) towed vertically through the water column at midday and midnight on six seasonal sampling time points (described below). Except for PAR data, midday and midnight CTD hauls were pooled as they were similar.

### Zooplankton vertical migration

To record vertical migration behavior in the loch, the mooring was equipped with two acoustic Doppler current profilers

(ADCP, Teledyne RD Instruments) pointing upward at 45 m and 120 m depth. The 300 kHz ADCPs have been extensively used to monitor mesozooplankton migrations (Tarling et al. 2002; Cottier et al. 2006; Brierley et al. 2006; Last et al. 2016). Acoustic data were checked for quality using the RDI correlation index (a measure of signal-to-noise ratio). Absolute backscatter volume (Sv, measured in decibel [dB]) was derived from echo intensity according to Deines (1999) with derived acoustic mean volume backscattering strength (MVBS).

### Field sample collection

Copepods were collected at Bonawe deep on six seasonal time points between May 2015 and March 2016 (Tables 1, 2). The time period was chosen to cover a single seasonal cycle of *C. finmarchicus* from animals born in April 2015 (Clark et al. 2013). All analyses were performed on the CV copepodid stage, the main overwintering stage that represents the bulk of the population over the year (Clark et al. 2013). Copepods were collected from the RV *Calanus* (Scottish Association for Marine Science [SAMS]) using a WP2-net equipped with an opening/closing mechanism (200  $\mu$ m mesh size/50  $\mu$ m cod end) hauled vertically through the water column. For all of the net hauls, the water column was separated into two layers with 5–50 m representing the “shallow” sample and 50–145 m representing the “deep” sample. The upper 5 m of the water column was excluded to avoid hypoosmotic stress of the animals due to surface brackish water (Fig. 2C). Community structure was determined from collections at midday and midnight and at both depths. Animals were fixed as bulk samples in 10% methanol for later analysis of *C. finmarchicus* abundance, life stage composition, and body length. It was assumed that sampling did not affect the stage composition as a mesh size of 200  $\mu$ m has been shown to catch at least 95% of the smallest copepodid stage CI and 100% of the older stages (Nichols and Thompson 1991). For each collected sample,  $n = 200$ –300 *C. finmarchicus* individuals were staged, and

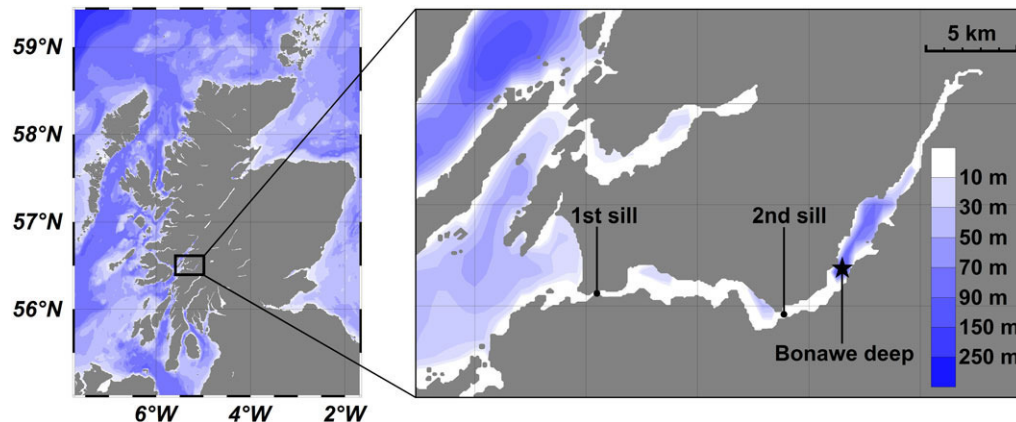


**Fig. 1.** Sampling site characteristics. Loch Etive is a sea loch at the western coast of Scotland, UK (56°45'N, 5°18'W). Water exchange with the ocean is limited by two sills. All samplings and the mooring deployment were done at the deepest point of the loch, Bonawe deep (~ 150 m), at the SAMS permanent station RE5. Maps were created with Ocean Data View v. 4.7.4 (Schlitzer 2015). Figure adopted and changed from Häfker et al. (2017).

**Table 1.** Collected samples. Listed samples were collected the same way at each seasonal time point. Sampling was always performed in two depth layers (5–50 m and 50–145 m, respectively) via vertical net hauls (see text). For each parameter, the time(s) of sampling, the number of collected replicates and sample handling are described. Only *C. finmarchicus* CV copepodids were used, except for abundance and stage composition where all copepodid life stages (incl. adults) were investigated.

| Parameter(s)                    | Time(s)          | n/depth layer                       | Sample handling  |
|---------------------------------|------------------|-------------------------------------|--|
| Abundance and stage composition | Midday, midnight | 2× 200–300 indiv.                   | Fixed in 10% methanol, sorted later                    |
| Body size                       |                  | 2× 100 CVs                          |  |
| Lipid content                   | Midday           | 5 (20 CVs/n)                        | Sorted under red light, fixed in liquid N <sub>2</sub> |
| Dry weight and C/N ratio        |                  | 24 (1 CV/n)                         |  |
| Gene expression                 | See Table 2      | 5 per diel time point (15–17 CVs/n) | Fixed in RNAlater <sup>®</sup> , sorted later          |

the length (from the tip of the head to the end of the furca) of  $n = 100$  CV copepodids was measured. Data for midday and midnight hauls were pooled for each seasonal time point and depth to avoid bias from DVM. In addition, animals collected at midday were sorted for *C. finmarchicus* CV copepodids using dissecting microscopes under dim red light and at in situ temperature and were then fixed in liquid nitrogen for later analyses of dry weight, carbon to nitrogen (C/N) ratio, and lipid content (see below). A summary of samples collected is presented in Table 1.

At each of the six seasonal time points, zooplankton samples were also collected over a period of 28 h at 4-h intervals with a total of eight diel time points per seasonal time point. Sampling at each seasonal time point started between 10:00 and 11:00 and ended between 14:00 and 15:00 on the following day (Table 2). The samples were immediately (within 1 min after retrieval) fixed as bulk samples in RNAlater<sup>®</sup> stabilizing solution (Ambion). The bulk samples were later sorted at 2°C for *C. finmarchicus* CV copepodids and for each depth layer,  $n = 5$  replicates were collected per diel time point with 15–17 individuals pooled per replicate and stored at –20°C for later gene expression analyses (see below). Upper Loch Etive represents a habitat of pure *C. finmarchicus* (as confirmed with population genetic studies, Søreide pers. comm.) and contamination of samples with the congener *Calanus helgolandicus* is highly unlikely due to its limited tolerance of low salinities (Hill 2009).

### Dry weight and C/N ratio

CV copepodids were individually fixed in pre-weighed tins in liquid nitrogen ( $n = 24$  per seasonal time point and depth, Table 1). They were then freeze dried and dry weight was determined (XP6U Micro Comparator, Mettler-Toledo). Afterward, the C/N ratio of the individuals was determined via elemental analyzer (EuroEA, EuroVector).

### Lipid analysis

Total lipid content of CV copepodids was determined over the seasonal sampling period. Replicates were taken for each seasonal time point and depth ( $n = 5$ ), with 20 individuals pooled per replicate (Table 1). Total lipid was extracted following Folch et al. (1957). Frozen copepods were initially homogenized in 4 mL chloroform : methanol (2 : 1 v/v) using a T10 ULTRA-TURRAX<sup>®</sup> disperser (IKA). The homogenate was then filtered through a pre-washed Whatman<sup>®</sup> N°1 filter (GE Healthcare). After the addition of 1 mL KCl (0.88% w/v), the samples were thoroughly homogenized using a vortex mixer before being centrifuged at  $400 \times g$  for 2 min for phase separation. After discarding the upper aqueous layer, the lower chloroform phase containing the total lipid extract was dried under a stream of oxygen-free nitrogen. The samples were then desiccated under vacuum for 6 h and total lipid mass [ $\mu\text{g} \cdot \text{indv.}^{-1}$ ] was determined gravimetrically.

**Table 2.** Diel time series sampling. Samples for gene expression analysis were collected at eight diel time points in 4-h intervals over a period of 28 h at each seasonal time point. Times of sunset, sunrise, and photoperiod at Bonawe deep were obtained from NOAA sunrise/sunset calculator. All times are given as UTC.

| Seasonal time point | Gene expression sampling period                       | Sunset | Sunrise | Photoperiod (h) |
|---------------------|---|--------|---------|-----------------|
| May 2015            | 6 <sup>th</sup> May 10:00–7 <sup>th</sup> May 14:00   | 20:12  | 04:24   | 15.8            |
| June                | 18 <sup>th</sup> Jun 10:00–19 <sup>th</sup> Jun 14:00 | 21:15  | 03:23   | 17.9            |
| August              | 5 <sup>th</sup> Aug 11:00–6 <sup>th</sup> Aug 15:00   | 20:24  | 04:33   | 15.9            |
| November            | 16 <sup>th</sup> Nov 11:00–17 <sup>th</sup> Nov 15:00 | 16:11  | 08:04   | 8.1             |
| January 2016        | 19 <sup>th</sup> Jan 11:00–20 <sup>th</sup> Jan 15:00 | 16:22  | 08:41   | 7.7             |
| March               | 3 <sup>rd</sup> Mar 10:00–4 <sup>th</sup> Mar 14:00   | 18:01  | 07:05   | 13.1            |

### Gene selection

Thirty five target genes and three reference genes were selected for analysis including genes involved in the circadian clock machinery, lipid-, carbohydrate- and amino acid metabolism, aerobic/anaerobic energy metabolism, stress response, and light perception. Sequences of relevant genes of interest from other crustaceans were used to browse a de novo transcriptome by Lenz et al. (2014) to identify respective gene sequences for *C. finmarchicus*. Clock genes had previously been annotated from the transcriptome (Christie et al. 2013a). The identities of the characterized sequences were verified via blastx using the NCBI online database. All measured genes, their physiological functions, and their respective blastx top-hits are listed in Supporting Information Table S1.

The sequence information obtained via blastx was then used to identify common protein domains and the sequences were further checked for palindromic regions and repeats using the online tools Oligoanalyzer 3.1 (<http://eu.idtdna.com/calc/analyzer>) and RepeatMasker 3.0 (<http://www.repeatmasker.org/cgi-bin/WEBRepeatMasker>). This identified suitable binding regions for primers and probes. Based on this information, custom Taqman® low-density array cards (Applied Biosystems) were designed via the Applied Biosystems online tool (<https://www.thermofisher.com/order/custom-genomic-products/tools/gene-expression/>) with primer and probe binding regions placed in sequence intersects specific to the respective gene (checked via blastn against NCBI). Cards were designed in a way that eight different samples could be measured in parallel with all 35 genes being measured in each sample. Sequences of primers and probes were submitted to the PANGAEA online repository (<https://doi.pangaea.de/10.1594/PANGAEA.884073>). Primer efficiencies were tested via dilution series and ranged from 83.8% to 104.0%.

### Gene expression analysis

To measure the expression of the selected genes, RNA was extracted using the RNeasy® Mini kit (Qiagen) with  $\beta$ -mercaptoethanol (0.14 M) added to the lysis buffer as recommended for lipid-rich samples. The TURBO DNA-free kit (Life Technologies) was used to remove genomic DNA and RNA was checked for possible degradation (2100 Bioanalyzer/RNA 6000 Nano Kit, Agilent Technologies) as well as for contaminants and overall RNA level (Nanodrop 2000 Spectrophotometer, Thermo Fisher Scientific). RNA yields per copepod determined via Nanodrop were used as a proxy for overall transcriptional activity. A thermocycler (T100 Thermal Cycler, Bio-Rad Laboratories) was used to convert 2  $\mu$ g RNA per sample (reaction volume: 50  $\mu$ L) to cDNA using RevertAid H Minus Reverse Transcriptase (Invitrogen). RNA samples were stored at  $-80^{\circ}\text{C}$  between all processing steps and cDNA was stored at  $-20^{\circ}\text{C}$ . Gene expression was measured via Taqman® cards (eight samples per card) and real-time quantitative PCR (ViiA™ 7, Applied Biosystems). Five cards were needed per

28-h time series (eight diel time points/ $n = 5$ ) and replicates of the same time point were separated between cards.

Gene expression was normalized using the  $2^{-\Delta\Delta\text{CT}}$ -method (Livak and Schmittgen 2001) with reference genes chosen based on expression level relative to investigated genes and the findings of previous studies (Hansen et al. 2008; Tarrant et al. 2008; Clark et al. 2013; Fu et al. 2013; Häfker et al. 2017). For the investigation of seasonal expression patterns, genes were normalized against the geometric mean of the reference genes *elongation factor 1  $\alpha$*  (*ef1 $\alpha$* ) and *ribosomal protein S13* (*rps13*) and the data of all samples collected during a 28-h time series at the respective seasonal time points were pooled (six seasonal time points,  $n = 40$  replicates per gene, seasonal time point and depth). For the investigation of diel expression cycles, the eight clock genes *clock* (*clk*), *cycle* (*cyc*), *period1* (*per1*), *period2* (*per2*), *timeless* (*tim*), *cryptochrome2* (*cry2*), *clockwork orange* (*cwo*), and *vri* (*vri*) were normalized against the geometric mean of the reference genes *rps13* and *RNA polymerase II* (*RNApoly*) and the 28-h time series from each of the different seasonal time points were treated individually (eight diel time points,  $n = 5$  replicates per gene, diel time point and depth). Expression stability of reference genes was verified via NormFinder (Andersen et al. 2004) with the geometric means of all used reference gene combinations showing stability values  $< 0.025$ .

### Statistical analysis

For the analysis of DVM patterns, backscatter rhythmicity of acoustic data from each seasonal sampling time point over the sampling period  $\pm 3$  days (7 days in total) for 25 m and 90 m depth was analyzed with TSA-Cosinor© (package 6.3, Expert Soft Technologies) and expressed as period length ( $\tau$ ) and % of model fit (Bingham et al. 1982).

All other statistical analyses were performed using RStudio (v. 0.99.442, R Development Core Team 2013). Graphics were created using SigmaPlot (v. 12.5) unless indicated otherwise. Seasonal patterns of body length, dry weight, C/N ratio, lipid content, and overall RNA level were analyzed separately for shallow and deep samples via nonparametric Kruskal–Wallis ANOVAs on ranks ( $\alpha = 0.05$ ) followed by Dunn’s multiple comparison post hoc tests ( $\alpha = 0.05$ ) provided in the “FSA” R-package (Ogle 2017). For each seasonal time point, a comparison between the shallow and the deep layer was made for all parameters using the Mann–Whitney *U*-test ( $\alpha = 0.05$ ).

Seasonal patterns of gene expression were analyzed the same way via Kruskal–Wallis ANOVAs on ranks and Mann–Whitney *U*-tests, but with  $\alpha = 0.0001$  to account for the testing of multiple genes (35 genes in 2 depth layers over 6 seasonal time points resulting in 70 Kruskal–Wallis ANOVAs and 210 Mann–Whitney *U*-tests). To identify reoccurring seasonal expression patterns, heatmaps, and dendrograms of all genes were created for the shallow and the deep layer with the R-packages “gplots” (Warnes et al. 2016) and “RColorBrewer” (Neuwirth 2014). For each depth, genes were then grouped

into four major clusters based on expression pattern similarities. Diel expression patterns of the eight clock genes over the 28-h time series were checked for 24-h cycling with the R-package “RAIN” (Thaben and Westermark 2014), which uses a non-parametric approach to detect rhythmic oscillations independent of waveform.  $\alpha = 0.001$  was used to account for the testing of multiple genes (8 genes in 2 depth layers resulting in 16 RAIN analyses). Cycling was analyzed separately for each seasonal time point as well as for the shallow and deep samples. The reference genes used for normalization (*rps13*, *RNA-poly*, and *ef1 $\alpha$* ) were excluded from all statistical analyses. All

other non-clock genes were also checked for 24-h rhythmicity, but none of them showed consistent diel patterns and thus data are not shown.

## Results

### Hydrography and primary production

Water temperature at Bonawe deep ranged between 8°C and 14°C over the course of the study. The temperature was most variable in the upper 60 m with lowest temperatures in winter/spring and the highest values at the end of the summer

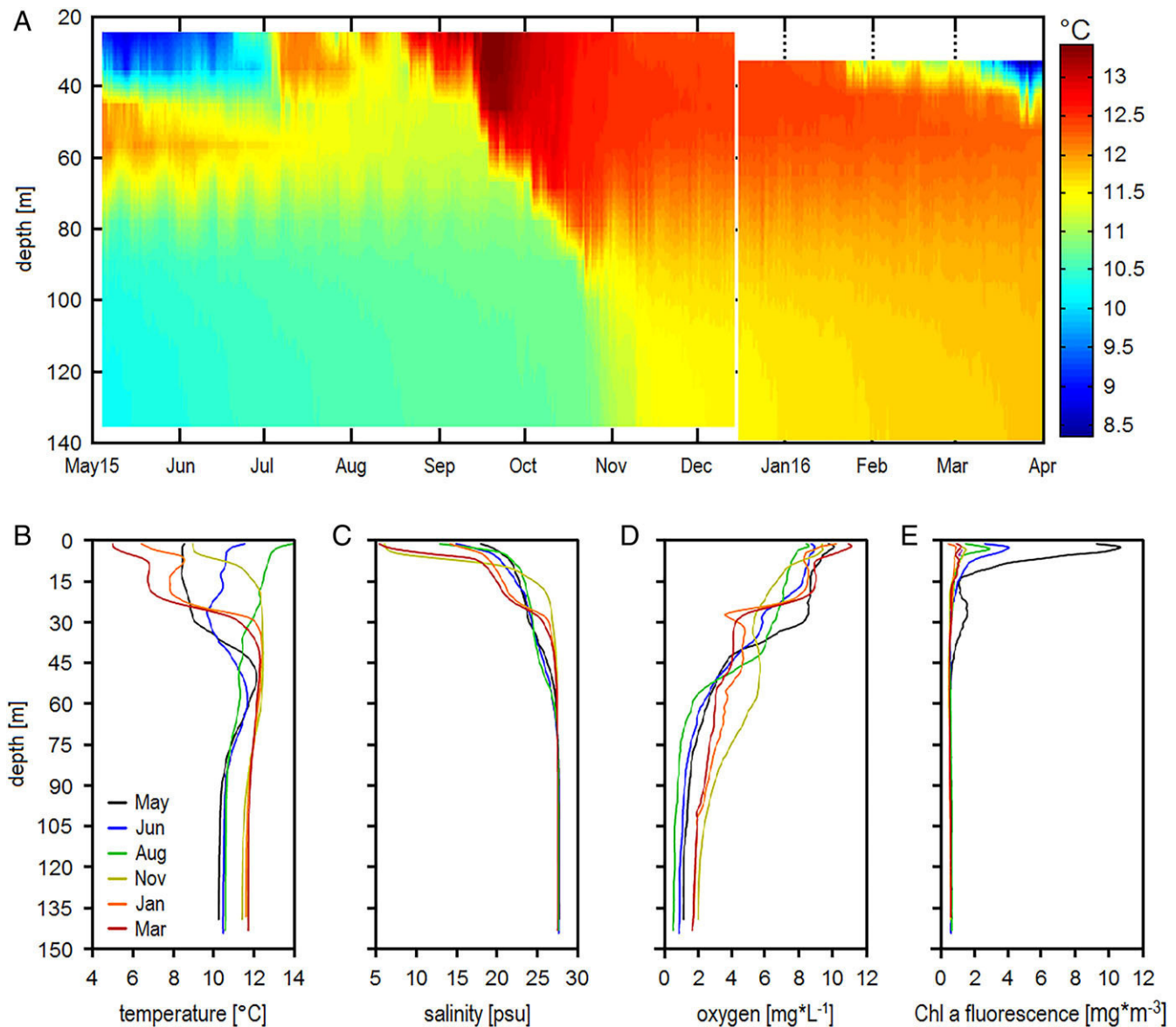


**Fig. 2.** Environmental parameters. Water column characteristics at the sampling site Bonawe deep were monitored. **(A)** Seasonal change in temperature recorded from loggers attached in 10 m intervals to a mooring. Date labels indicate the 1<sup>st</sup> day of the respective month. The gap in December resulted from the temporary retrieval of the mooring for maintenance and data collection. CTD hauls additionally provided high resolution profiles of **(B)** temperature, **(C)** salinity, **(D)** oxygen concentration, and **(E)** Chl *a* concentration for each seasonal time point. CTD data for May were previously shown in Häfker et al. (2017).

(Fig. 2A,B). Below 80 m, the temperature rose by  $\sim 1^\circ\text{C}$  in November/October followed by a weak gradual warming that continued until March. Salinity generally increased with depth and was stable at 27.5 PSU below  $\sim 60$  m throughout the study period. A sharp decrease to 13–18 PSU was observed in the upper 5 m and from January to March salinity already decreased to  $\sim 22$  PSU at 20–30 m depth (Fig. 2C). Oxygen concentration decreased with depth and the largest changes occurred between 10 m and 50 m, with an especially sharp decrease in January and March at 20–30 m depth (Fig. 2D). According to the Chl *a* data, phytoplankton was concentrated in the upper 10 m of the water column with a second, weaker peak at  $\sim 25$  m in May. The Chl *a* maximum in May ( $10.5 \text{ mg Chl } a \cdot \text{m}^{-3}$ ) was followed by a sharp decrease until August (Fig. 2E), while from November to March the phytoplankton abundance was very low ( $< 1.5 \text{ mg Chl } a \cdot \text{m}^{-3}$ ). Midday PAR at 1 m depth varied between  $\sim 100 \mu\text{mol photons} \cdot \text{m}^{-2} \cdot \text{s}^{-1}$  in

May–August and  $\sim 10 \mu\text{mol photons} \cdot \text{m}^{-2} \cdot \text{s}^{-1}$  in November/January, but was strongly affected by weather conditions (cloud cover) during the sampling trips. Generally, light intensity decreased rapidly with depth and was no longer detectable below 20 m at any seasonal time point (sensor detection limit:  $1 \times 10^{-12} \mu\text{mol photons} \cdot \text{m}^{-2} \cdot \text{s}^{-1}$ ).

### Zooplankton diel vertical migration

Classical DVM was observed at the study site with animals migrating to the surface at night and retreating to deeper waters during the day. Times of upward/downward migration generally coincided with sunset/sunrise (Fig. 3A). In shallow waters (measured at 25 m), 24-h backscatter rhythmicity could be detected at all seasonal sampling time points, while in the deeper layer (measured at 90 m) a diel backscatter rhythm was only found in May and June (Table 3). Migrations stretched from the surface to  $\sim 70$  m depth in May/June and became

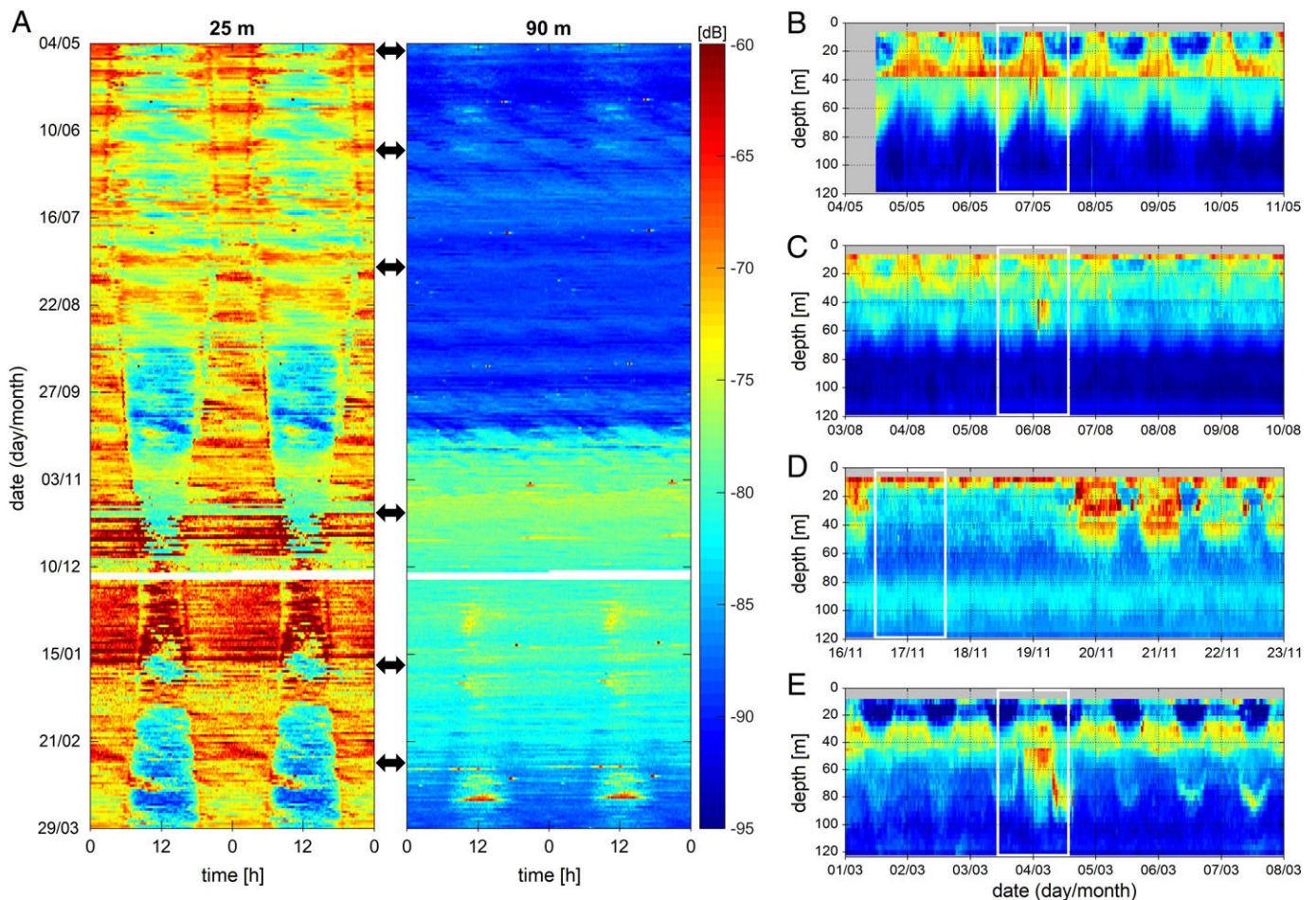


**Fig. 3.** Diel vertical migration patterns at Bonawe deep, Loch Etive. MVBS, expressed in (dB) is shown. **(A)** Diel change in MVBS at 25 m and 90 m, respectively. Data are double plotted. Arrows ( $\leftrightarrow$ ) indicate seasonal sampling time points. The gap in December resulted from the temporary retrieval of the mooring for maintenance and data collection. **(B–E)** MVBS patterns recorded over 7 day periods around the seasonal sampling time points in May, August, November, and March, respectively. Date labels at 00:00 h of the respective day. The times of the 28-h sampling campaigns are indicated by white boxes. The sharp change in backscatter at  $\sim 38$  m (particularly strong in May) is an artifact caused by the combination of data from two ADCPs at different depths. MVBS pattern for May **(B)** was previously shown in Häfker et al. (2017).

**Table 3.** Zooplankton backscatter rhythmicity over the course of the study. Data obtained via ADCP set to a frequency of 300 kHz. For each seasonal time point the oscillation period ( $\tau$ ) and fit were determined by TSA Cosinor analysis over a period of 7 days. Data for May were previously shown in Häfker et al. (2017).

| Seasonal time point       | Shallow (25 m)    |             | Deep (90 m)       |             |
|---------------------------|-------------------|-------------|-------------------|-------------|
|                           | Period ( $\tau$ ) | % Model fit | Period ( $\tau$ ) | % Model fit |
| May (04.–11.05.2015)      | 23.9              | 49.6        | 24.0              | 33.3        |
| June (15.–22.06.2015)     | 24.1              | 52.7        | 23.6              | 16.8        |
| August (03.–10.08.2015)   | 23.8              | 20.7        | –                 | –           |
| November (09.–16.11.2015) | 24.1              | 41.2        | –                 | –           |
| January (19.–26.01.2016)  | 24.0              | 40.6        | –                 | –           |
| March (01.–08.03.2016)    | 23.8              | 62.7        | –                 | –           |

shallower afterward (Fig. 3B–D). In January/March, animals did not migrate all the way to the surface but accumulated at ~ 30 m depth at night (Fig. 3E).

### C. finmarchicus population dynamics

Overall, *C. finmarchicus* abundance in the shallow layer (5–50 m) was highest in May (453 indiv.\*m<sup>-3</sup>) followed by August (147 indiv.\*m<sup>-3</sup>) (Fig. 4A), while in June and from November to March it was below 75 indiv.\*m<sup>-3</sup>. In the deep layer (50–145 m), abundance gradually increased from a minimum in May (27 indiv.\*m<sup>-3</sup>) to high abundances in November (220 indiv.\*m<sup>-3</sup>) and January (197 indiv.\*m<sup>-3</sup>) and then decreased to 75 indiv.\*m<sup>-3</sup> in March (Fig. 4B).

In the shallow layer, from May to August, early copepodid stages (CI–CIV) accounted for more than 60% of the

*C. finmarchicus* population. The remaining population consisted of CVs and adults (mostly females) with the former outnumbering the latter (Fig. 4A). By November, CVs made up ~ 60% of the shallow population and they stayed dominant until the end of the study, although in March the proportion of adults did again increase to ~ 35%. The deep layer was dominated by adult females (~ 65%) in May, but from June onward until the end of the study almost the entire deep population (> 95%) consist of CV copepodids (Fig. 4B).

### Body length, dry weight, C/N ratio, and lipid content

Body length of the CV copepodids showed significant seasonal differences in both depth layers (Kruskal–Wallis  $p < 0.05$ ,  $df = 5$ ) (Fig. 5A). In the shallow layer, CV body length decreased from ~ 2.9 mm in May/June to 2.7–2.75 mm from August to March. A similar pattern was observed in the deep layer, but with the major decrease between August and November. While shallow CVs were significantly bigger in May, deep layer animals were bigger from August on (Mann–Whitney  $U$ -test,  $p < 0.05$ ). A more detailed analysis of CV copepodid individual sizes is provided in Supporting Information Fig. S1.

Dry weight of the CV copepodids varied between 100  $\mu\text{g}$  and 260  $\mu\text{g}$  individual<sup>-1</sup> and showed a significant seasonal change in both depths (Kruskal–Wallis  $p < 0.05$ ,  $df = 5$ ). In the shallow layer, dry weight decreased from June to November followed by an increase toward January/March (Fig. 5B). Dry weight of CVs from the deep layer peaked in August and then decreased to a minimum in January. In August, November, and March copepods from the deep layers had a significantly higher mass than those from the shallow layers (Mann–Whitney  $U$ -test,  $p < 0.05$ ).

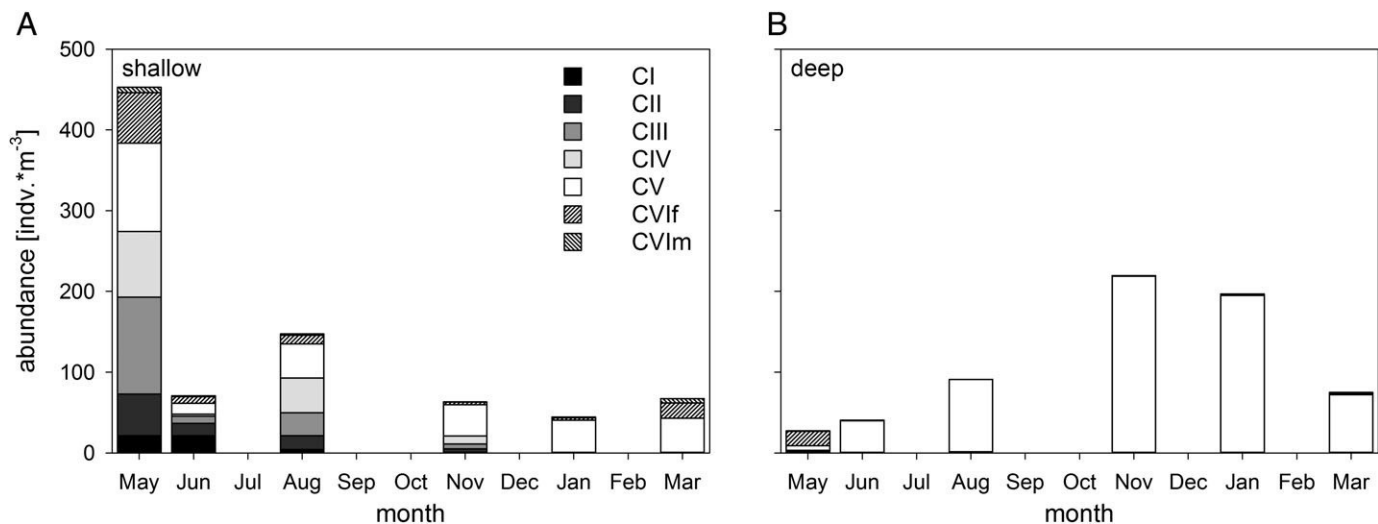


**Fig. 4.** *C. finmarchicus* abundance and stage composition. Samples were collected at Bonawe deep via vertical net hauls in (A) the shallow layer and (B) the deep layer. Copepodid stages (CI–CV) and adults (CVIf, CVIm) were counted. At each seasonal time point samples were collected at midday and midnight and data were pooled to prevent DVM effects. For months without bars, no samples were collected.

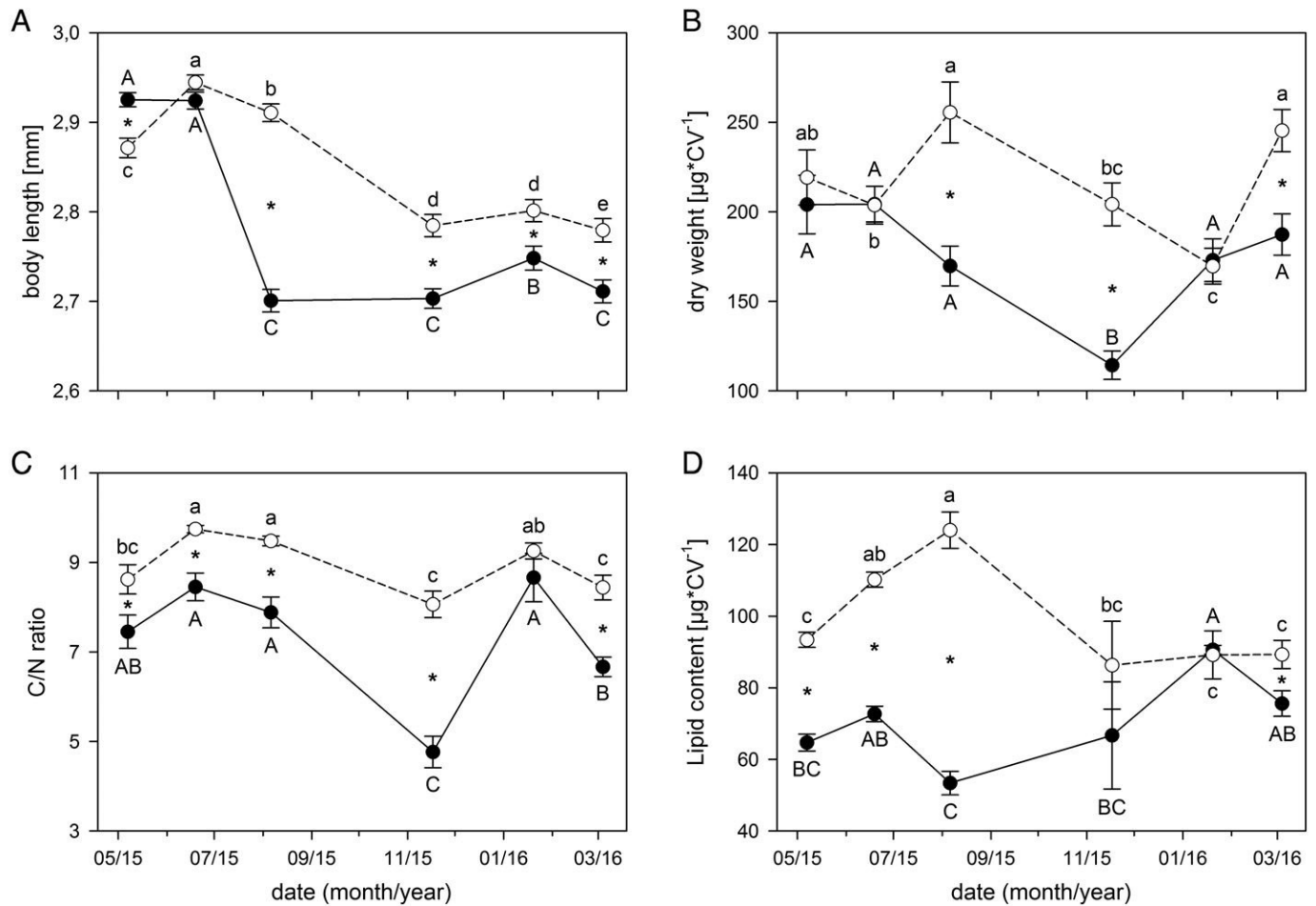


**Fig. 5.** Body condition parameters. Changes in (A) body length, (B) dry weight, (C) C/N ratio, and (D) total lipid content of *C. finmarchicus* CV copepodids in the shallow layer (solid symbols and line) and the deep layer (open symbols, dashed line) are shown. Date labels indicate the 1<sup>st</sup> day of the respective month. Significant seasonal differences within depth layers were identified via Kruskal–Wallis ANOVA and are indicated by different capital letters for the shallow layer and different lower case letters for the deep layer, respectively. Significant differences between the shallow and deep layer at each seasonal time point were identified via Mann–Whitney *U*-test and are indicated by an asterisk (\*) between the symbols at the respective time points. For each depth layer and seasonal time point, the number of replicates measured was  $n = 100$  for body length,  $n = 24$  for dry weight,  $n = 24$  for C/N ratio, and  $n = 5$  for total lipid content. Mean values  $\pm$  standard error are shown.

The C/N ratio of CV copepodids changed significantly over the seasonal cycle with similar patterns in both depth layers (Kruskal–Wallis  $p < 0.05$ ,  $df = 5$ ). Changes were largest in the shallow layer with highest C/N values around 8 in June, August, and January, while the ratio decreased to 4.77 in November and 6.67 in March (Fig. 5C). C/N ratios in the deep layer were significantly higher than in the shallow layer for all seasonal time points except January (Mann–Whitney *U*-test,  $p < 0.05$ ).

Significant seasonal changes in total lipid content of copepods from both the shallow and the deep layer were found (both Kruskal–Wallis  $p < 0.05$ ,  $df = 5$ ) (Fig. 5D). In the shallow layer, total lipid content per individual CV copepodid varied from 53  $\mu\text{g}$  in June to  $\sim 80 \mu\text{g}$  in January/March. In the deep layer, CV lipid content increased from 93  $\mu\text{g}$  in May to 124  $\mu\text{g}$  in August and was constant at  $\sim 90 \mu\text{g}$  from November on. The lipid content of CVs in the

deep layers was higher than in the shallow layer from May to August and in March (Mann–Whitney *U*-test,  $p < 0.05$ ). Both depth layers showed high variability in lipid content in November.

### Seasonal gene expression

RNA yield per copepod in *C. finmarchicus* CVs was highest in May for both depths (Kruskal–Wallis  $p < 0.05$ ,  $df = 5$ ) and, with the exception of November, was generally higher in the shallow layer (Mann–Whitney *U*-test,  $p < 0.05$ ) (Fig. 6). In the shallow layer, the RNA yield showed a minimum in November with a slight increase thereafter. In the deep layer, RNA yield reached a minimum in August and stayed constantly low thereafter.

Almost all of the investigated genes showed significant seasonal expression changes in both depth layers (Kruskal–Wallis  $p < 0.0001$ ,  $df = 5$ , Supporting Information Table S2).

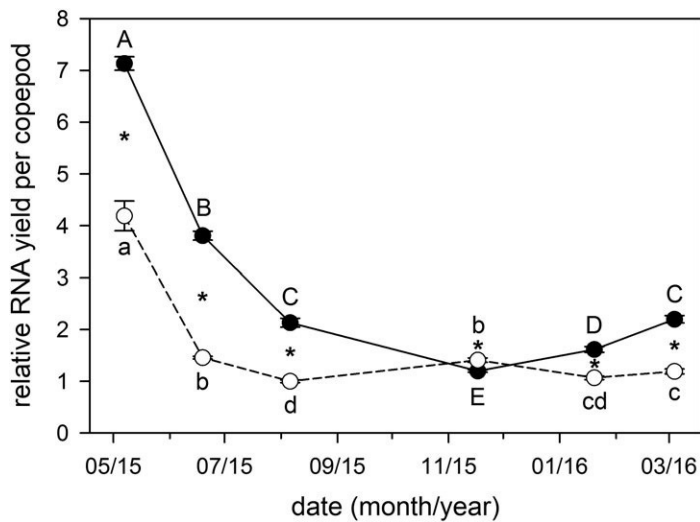


**Fig. 6.** RNA yield per copepod. Relative seasonal change of RNA content of *C. finmarchicus* CV copepodids in the shallow layer (solid symbols and line) and the deep layer (open symbols, dashed line) is shown. Date labels indicate the 1<sup>st</sup> day of the respective month. Statistical analyses and labeling were performed as described for Fig. 5. For each depth layer and seasonal time point  $n = 40$  replicates were measured. Mean values  $\pm$  standard error are shown.

The Mann–Whitney  $U$ -tests found numerous significant differences between the shallow and deep layer for various genes and seasonal time points ( $p < 0.0001$ , Supporting Information Table S2). The number of genes differing significantly in expression between the shallow and deep layer varied with season. The number was lowest in May and November (11 and 15 genes, respectively) and highest in June and August (25 and 28 genes, respectively). Relative change in seasonal expression level was variable among genes, ranging from 1.6-fold change for *citrate synthase* (*cs*) to 68-fold change for *chymotrypsin* (*chtrp*) and even 5477-fold change for *elongation of very long fatty acids protein* (*elov*). For 21 of 35 investigated genes, the maximum change was between twofold and 10-fold (Supporting Information Table S2).

Heatmap analyses of gene expression revealed several clusters of reoccurring seasonal patterns. In the shallow layer, there were four distinctive clusters (Fig. 7A) with the first one ( $S_1$ ) characterized by elevated expression from May to August, a minimum in November and an increase toward high expression in March. Genes in the  $S_1$  cluster included among others: *cs*, *malate dehydrogenase* (*mdh*), *cyclin B* (*cyclB*), and *ecdysteroid receptor* (*ecr*) as well as the clock-associated genes like *cryptochrome1* (*cry1*) and *casein kinase II  $\alpha$*  (*ck2a*). The second cluster ( $S_2$ ) showed consistent peak activity in May or sometimes June, followed by a gradual or stepwise decrease toward the lowest values in March. Genes in the  $S_2$  cluster included *elov*, *phosphofructokinase* (*pfk*), *chtrp*, and *glutamate dehydrogenase* (*gdh*) as well as the clock genes *cyc*, *per2*, and *cwo*. The third cluster ( $S_3$ ) showed no clear seasonal patterns and consisted of

the genes *phosphoenolpyruvate carboxykinase* (*pepck*), *widerborst* (*wbt1*), and the clock gene *vri*. The fourth shallow layer cluster ( $S_4$ ) was characterized by an expression peak in November, minimum values in March, and consistently low expression in the remaining months. Representatives of the  $S_4$  cluster were *hemocyanin* (*hc*), *ferritin* (*fer*), *couch potato* (*cpo*), *arginine kinase* (*argk*), an opsin (*ops*), and the clock genes *per1*, *tim*, and *cry2*.

In the deep layer, the heatmap analysis identified four distinctive clusters (Fig. 7B). In the first cluster ( $D_1$ ), expression was high in May, largely reduced from June until November and then increased again to initial levels in March. The cluster composition shared large similarity with the  $S_1$  cluster of the shallow layer and included the genes *cs*, *mdh*, *cyclB*, *ecr*, *cry1*, and *ck2a*. Comparing  $D_1$  and  $S_1$ , expression was similar between depths in May, November, and March while expression was higher in the shallow layer in June, August, and January (Supporting Information Table S2). The second cluster of the deep layer ( $D_2$ ) was characterized by peak expression in May followed by a sharp decline to low levels in June/August and thereafter. The genes of the  $D_2$  cluster (including *elov*, *pfk*, and *chtrp*) were all found in the  $S_2$  cluster of the shallow layer. Individual gene comparison of  $D_2$  and  $S_2$  revealed higher expression in the shallow layer from May to November with the difference between depths gradually decreasing (Supporting Information Table S2). Genes of the third deep layer cluster ( $D_3$ ) all showed peak expression in June followed by a sharp or gradual decrease and often low expression in May. The  $D_3$  cluster included *pepck*, *pigment dispersing hormone receptor* (*pdhr*), and the clock genes *cyc*, and *vri* that were found in the  $S_2$  and  $S_3$  clusters of the shallow layer. Expression of individual genes was similar between the deep and shallow layer for most of the study period, with some genes showing higher expression in the deep layer from June to November (Supporting Information Table S2). The fourth cluster of the deep layer ( $D_4$ ) was characterized by high expression levels from June to November and low expression levels in May and March. Most genes of the  $D_4$  cluster were found in the  $S_4$  cluster of the shallow layer (including *hc*, *fer*, *cpo*, *argk*, *ops*, *per1*, *tim*, and *cry2*), while a few like *3-hydroxyacyl-CoA dehydrogenase* (*hoad*) and *clk* were found in the  $S_2$  cluster. Expression was similarly low in the  $D_4$  and the  $S_4$  cluster in May and March, but most genes showed higher expression levels in the deep layer from June to January compared to the shallow layer (Supporting Information Table S2).

#### Diel clock gene expression

The diel rhythmicity of the clock genes *clk*, *per1*, *tim*, *cry2*, and *cwo* showed similar changes over the seasonal cycle. 24-h cycling of these genes was mostly confined to the shallow layer from May to August (Table 4). In the deep layer, 24-h cycling (if present) was reduced with *tim* and *cwo* being

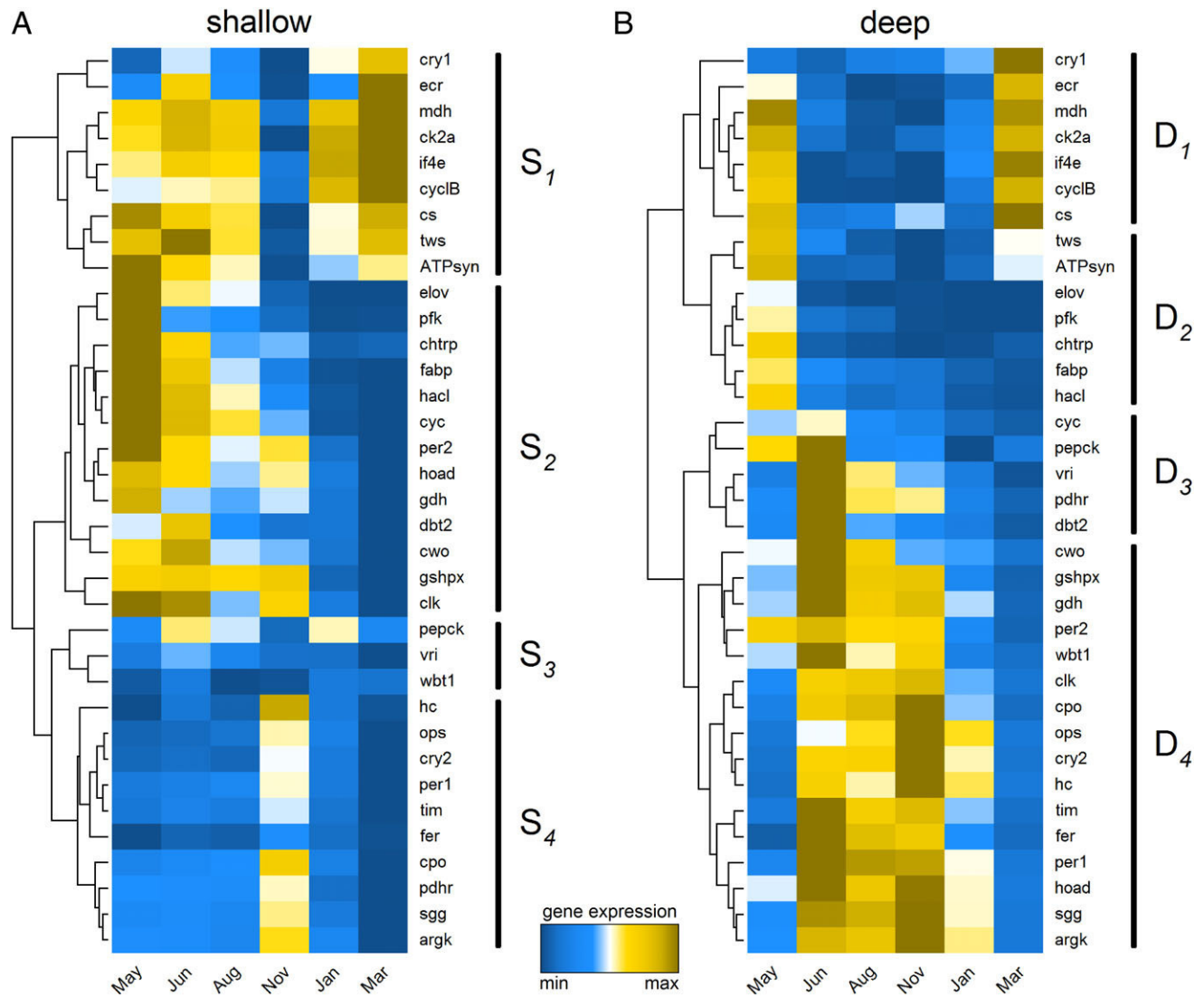


**Fig. 7.** Seasonal gene expression patterns. (A) Shallow and (B) deep layer gene expression heatmaps and clusters are shown. Gene clusters were defined based on pattern similarities. Gene expression of both depth layers was normalized individually for each gene, meaning that relative expression levels are comparable between months and depth layers but not between genes. A detailed overview of expression differences between months and depths layers is given in Supporting Information Table S2. Graphic was created with R.

rhythmic in May, while only *cyc* was rhythmic in June. From May to August, *clk* typically showed peak expression just after sunrise (Fig. 8A). In contrast, the diel expression peak of *per1*, *tim*, *cry2*, and *cwo* typically peaked around sunset (Fig. 8B–E). The clock genes *cyc*, *per2*, and *vri* showed generally little 24-h cycling and no consistent diel patterns over the seasonal cycle (graphics not shown).

## Discussion

This study has generated one of the most comprehensive investigations of *C. finmarchicus*' seasonal cycles to date. The multilevel approach revealed seasonal rhythms of DVM, population dynamics, as well as the physiology, gene expression, and clock rhythmicity of the dominant CV life stage. Initial

discussion will focus on seasonal changes in DVM followed by a detailed characterization of the three distinct phases in the seasonal cycle of *C. finmarchicus* CV copepodids: (1) activity/development (shallow layer, May–October), (2) diapause (deep layer, June–November), and (3) emergence (November–March). All phases show specific patterns of physiology, gene expression, and clock rhythmicity (Fig. 9). Finally, observed patterns of circadian clock rhythmicity and lipid content will be discussed in relation to photoperiod and possible regulatory mechanisms of diapause initiation/termination.

## Diel vertical migration

DVM showed 24-h rhythmicity throughout the study and, the times of zooplankton ascent and descent in Loch Etive

**Table 4.** Diel cycling in clock gene expression. *p* values of “RAIN” rhythm analysis are shown with *p* values indicating significant 24-h cycling ( $p < 0.001$ ) printed bold. For the sake of clarity, *p* values  $> 0.05$  are not shown (–). Data for May were previously shown in Häfker et al. (2017).

| Gene                          | Depth   | Rhythm analysis (24-h, $\alpha = 0.001$ ) |                  |                  |                  |         |                  |
|-------------------------------|---------|---|------------------|------------------|------------------|---------|------------------|
|                               |         | May                                       | June             | August           | November         | January | March            |
| <i>clock (clk)</i>            | Shallow | <b>&lt;0.001</b>                          | <b>&lt;0.001</b> | 0.016            | –                | –       | <b>&lt;0.001</b> |
|                               | Deep    | –   | –                | –                | –                | –       | –                |
| <i>cycle (cyc)</i>            | Shallow | –   | 0.023            | –                | –                | –       | –                |
|                               | Deep    | –   | <b>&lt;0.001</b> | –                | –                | –       | –                |
| <i>period1 (per1)</i>         | Shallow | <b>&lt;0.001</b>                          | 0.005            | <b>&lt;0.001</b> | –                | –       | –                |
|                               | Deep    | 0.027                                     | 0.014            | –                | –                | –       | –                |
| <i>period2 (per2)</i>         | Shallow | –   | –                | –                | –                | –       | –                |
|                               | Deep    | 0.005                                     | –                | –                | –                | –       | –                |
| <i>timeless (tim)</i>         | Shallow | <b>&lt;0.001</b>                          | 0.023            | <b>&lt;0.001</b> | –                | –       | 0.050            |
|                               | Deep    | <b>&lt;0.001</b>                          | –                | –                | –                | –       | –                |
| <i>cryptochrome2 (cry2)</i>   | Shallow | <b>&lt;0.001</b>                          | 0.007            | <b>&lt;0.001</b> | –                | 0.005   | –                |
|                               | Deep    | –   | –                | –                | –                | –       | –                |
| <i>clockwork orange (cwo)</i> | Shallow | <b>&lt;0.001</b>                          | <b>&lt;0.001</b> | <b>&lt;0.001</b> | –                | –       | 0.005            |
|                               | Deep    | <b>&lt;0.001</b>                          | –                | 0.004            | –                | –       | –                |
| <i>vriille (vri)</i>          | Shallow | –   | –                | 0.002            | <b>&lt;0.001</b> | –       | –                |
|                               | Deep    | –   | 0.018            | –                | –                | –       | –                |

coincided with sunset and sunrise and shifted over the seasons according to photoperiod (Fig. 3; Table 2), with shoaling of DVM in autumn/winter. This supports the general assumption that DVM is synchronized by light. The observed patterns were primarily attributed to *C. finmarchicus*, the dominant zooplankton species in Loch Etive (Mauchline 1987; Hill 2009) and in our net catches. However, in autumn/winter, while the majority of *C. finmarchicus* were diapausing in the deep layer (Fig. 4), other zooplankton species like the large predatory copepod *Paraeuchaeta norvegica* or the chaetognath *Parasagitta elegans* might have contributed to the observed DVM patterns (Mauchline 1987). Light intensity in Loch Etive decreased rapidly with depth because of the river input of humic compounds (Wood et al. 1973). PAR data suggest that at any seasonal time point light was undetectable for *C. finmarchicus*, and probably most zooplankton organisms, below 20 m depth (Båtnes et al. 2013; Miljeteig et al. 2014; Cohen et al. 2015). Daytime backscatter was strongest at 40–60 m depth, suggesting that the ascent to the surface at sunset was not triggered by light but rather by internal cues like hunger or endogenous clocks. In March, a pronounced cline due to freshwater runoff (Fig. 2B–D) prevented zooplankton from ascending above 30 m depth (Fig. 3E), meaning that they spend the entire 24-h cycle in constant darkness and still showed synchronized DVM. This strongly suggests an endogenous regulation of zooplankton DVM (Enright and Hamner 1967; Cohen and Forward 2005; Häfker et al. 2017). Such endogenous DVM is also supported by reports of rhythmic migrations during the polar night and in deep sea habitats (Berge et al. 2009; van Haren and Compton 2013).

### Seasonal life cycle of *C. finmarchicus*

#### Activity and development phase

Spring and summer in the shallow layer were characterized by *C. finmarchicus* early copepodid stages, high metabolic activity, and diel rhythmicity. The first generation ( $G_1$ ) sampled in May/June were the offspring of the overwintering stock. One fraction of the  $G_1$  descended to diapause whereas the other fraction matured and spawned a second generation ( $G_2$ ), which was sampled in August. The presence of a second generation from August on was inferred from the decrease in body length, dry weight, and lipid content of the shallow layer CV copepodids from June to August (Fig. 5, Supporting Information Fig. S1). This finding was surprising as previous investigations in Loch Etive reported only one generation per year (Hill 2009) and it may be linked to nutrient enrichment from increasing fin-fish aquaculture in the loch in the last few years. The descent of the  $G_1$  and the  $G_2$  to diapause occurred around June and October, respectively. The descent of the  $G_1$  is mostly reflected in the abundance data from the shallow and deep layers in June/August (Fig. 4) and the change in deep layer gene expression patterns (Fig. 8B). *C. finmarchicus* abundance in net samples collected in the shallow and deep layers for physiological and genetic analyses support the suggestion that a major relocation of biomass (i.e., of the  $G_1$ ) to the deep layer already occurred in June. The descent of the  $G_2$  becomes evident from the backscatter increase at depth in October (Fig. 3A, 90 m) as well as from the appearance of smaller sized CV copepodids in the deep layer in November (Supporting Information Fig. S1) and it seems to be associated with an increase in water temperature. A similar temperature-related

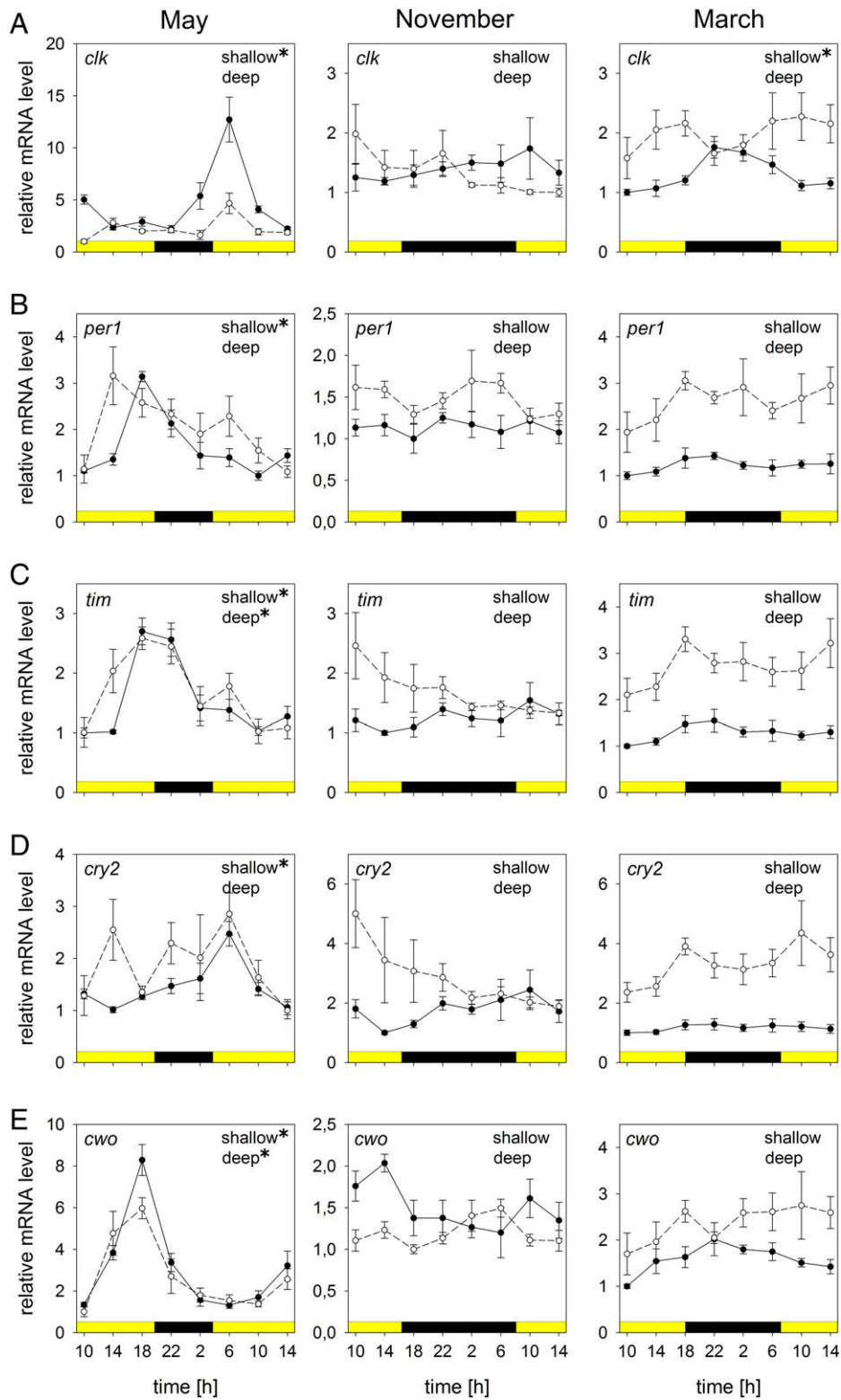


**Fig. 8.** Diel clock gene expression patterns. Relative mRNA levels of (A) *dock/clk*, (B) *period1/per1*, (C) *timeless/tim*, (D) *cryptochrome2/cry2*, and (E) *clockwork orange/cwo* are shown for the months May, November, and March in the shallow (solid symbols and line) and in the deep layer (open symbols, dashed line). Color bars indicate day/night. For each gene, depth layer, and diel time point  $n = 5$  replicates were measured. Mean values  $\pm$  standard error are shown. Gene expression was normalized individually for each month, meaning that relative expression levels are comparable between depth layers but not between months or genes. All genes were checked for rhythmic gene activity using the R-Package “RAIN” and significant 24-h cycling is indicated by asterisks (\*). Information about the cycling of other clock genes and months is presented in Table 4. Expression patterns for May were previously shown in Häfker et al. (2017).

seasonal migration has been observed in *C. finmarchicus*' congener *C. glacialis* (Kosobokova 1999; Niehoff and Hirche 2005) (Fig. 2A).

From May to August, gene expression patterns indicate high metabolic activity and active development of the copepods in the shallow layer (Fig. 7A  $S_1$ – $S_4$ ). In the  $S_1$  cluster, high expression was found in genes associated with metabolic activity like *mdh* or *cs* (Meyer et al. 2002, 2010; Freese et al. 2017), translation activity (*initiation factor 4E* [*if4E*]), molting (*ecr*), and tissue development (*cyclB*). The  $S_2$  gene cluster also showed high expression during the phase of activity and development and especially in May, i.e., the time when the phytoplankton concentration peaked (Fig. 2E). Many  $S_2$  genes are involved in feeding-related processes such as digestion (*chtrp*), the channeling of carbohydrates (*pfk*), and nitrogen compounds (*glutamate dehydrogenase* [*gdh*]) into the citric acid cycle as well as in the synthesis of lipid reserves (*elov* and *fatty acid-bind protein* [*fabp*]). High expression levels were further found in *hydroxyacyl-CoA lyase* (*hacl*), an enzyme which catabolizes the  $\alpha$ -oxidation of consumed fatty acids in the peroxisomes (Casteels et al. 2007). It thus seems likely that expression of several  $S_2$  genes could be affected by ambient food conditions. Genes in the  $S_3$  and  $S_4$  clusters showed low expression levels from May to August, suggesting that they play a reduced role during the phase of activity and development. The clock genes *per1*, *tim*, and *cry2* were found in the  $S_4$  cluster indicating that high clock gene expression levels are not necessarily an indicator of clock rhythmicity.

The strong diel cycling of clock genes in the shallow layer from May to August (Fig. 8; Table 4) indicates a functioning circadian clock, which is probably also coordinating diel rhythms in behavior (e.g., DVM) and physiology. The diel expression of the clock genes mostly resembles the patterns previously reported for *C. finmarchicus* (Häfker et al. 2017) and other arthropod species (Richier et al. 2008; Merlin et al. 2009) (Fig. 8). No coincidence was seen in the expression of clock genes and the seasonal changing photoperiod suggesting that photoperiodic measurement may be achieved via an "external coincidence" model (Bünning 1960; Pittendrigh 1960). This proposes a photosensitive phase around sunset or sunrise associated with peak activity of one or more clock genes. However, the sampling interval (4 h) was too long to reliably test for this model. While 24-h cycling was only found in clock genes but not in any other genes, it is probable that the clock also controls diel physiological rhythms such as respiration (Häfker et al. 2017) or enzyme activity associated with nocturnal feeding (Båmstedt 1988) via downstream genes that then trigger cellular signal cascades regulating metabolic processes (Ceriani et al. 2002; Panda et al. 2002). These cascades may influence protein synthesis or enzyme activity (Panda et al. 2002; Reddy and Rey 2014; Thurley et al. 2017) explaining the lack of diel cycles in metabolic gene expression. To fully reveal the extent and organizational levels of circadian control in *C. finmarchicus*, circadian transcriptome and

proteome studies will be needed. Interestingly, several clock genes (*clk*, *cyc*, *per2*, and *cwo*) showed a clear change in expression level from May to August, but diel clock rhythmicity was not affected (Table 4), suggesting that the clock can maintain robust 24-h rhythmicity even if overall clock gene expression levels change.

### Diapause phase

*C. finmarchicus* typically diapauses as a CV copepodid (Marshall and Orr 1955; Hirche 1996a), which dominated the deep layer from June to March in this study. Some copepods of the  $G_1$  already descended to diapause in May as indicated by the presence of lipid-rich CV copepodids in the deep layer at this time. The descent of the  $G_2$  in October was accompanied by a decrease in deep layer average CV body length and dry weight (Fig. 5A,B, Supporting Information Fig. S1).

According to gene expression in May and June, the physiological "switch" to diapause took place after the descent to the deep layer, as previously suggested (Head and Harris 1985; Freese et al. 2017). Diapausing copepods were characterized by high expression of genes in the  $D_3$  and  $D_4$  clusters, suggesting that the diapause phase lasted from June until after November (Fig. 7B). The genes with low expression in the  $D_1$  and  $D_2$  clusters were related to metabolic activity, development, and food processing (e.g., *mdh*, *cyclB*, and *chtrp*) as well as molting (*ecr*) and lipid synthesis (*elov* and *fabp*) (Fig. 7B), which is in line with previous findings in diapausing *C. finmarchicus* (Tarrant et al. 2008; Aruda et al. 2011; Clark et al. 2013).

Genes in the  $D_3$  cluster showed highest expression in June, suggesting an association with the initiation of diapause (e.g., *pepck* and *pigment dispersing hormone receptor* [*pdhr*]). High expression of *pepck*, the rate-limiting enzyme of gluconeogenesis, suggests an increase of anaerobic energy production (Hahn and Denlinger 2011; Poelchau et al. 2013) as a consequence of the hypoxic conditions in the deep layer (Fig. 2D). This may be fueled by glucose produced from lipid sac wax esters via gluconeogenesis and then distributed within the body, but only experimental exposure to hypoxia and tissue-specific gene expression analysis would shed new light onto the role of *pepck* in diapausing *C. finmarchicus*. *pdhr* is involved in reducing the sensitivity to light (Strauss and Dirksen 2010) and the high *pdhr* expression in June might be associated with the transition to diapause as light can trigger arousal in *Calanus* (Miller et al. 1991; Morata and Søreide 2013). For the  $S_3$  cluster genes, closer investigations of their molecular and physiological roles will be needed to determine if and how they are involved in diapause initiation.

The  $D_4$  cluster contained several genes typically associated with overwintering such as *cpo*, which is linked to diapause in insects (Christie et al. 2013b; Salminen et al. 2015) or *hoad*, which is a key enzyme of lipid catabolism (Hassett et al. 2010). Other upregulated genes are involved in blood oxygen supply (*hc*), anaerobic energy production (*argk*), or in the protection from oxidative stress (*gshpx* and *fer*). Elevated

expression of *fer* in deep diapausing *C. finmarchicus* has already been described (Tarrant et al. 2008; Aruda et al. 2011) and is intuitive considering that hypoxia can cause oxidative stress (Chandel et al. 2000). However, while the oxygen concentration was constantly low in the deep layer of Loch Etive (Fig. 2D), expression in the D<sub>4</sub> cluster was only elevated from June to November/January, suggesting that the observed changes were directly associated with diapause and possibly related to the reduced oxygen and ATP demands due to metabolic reduction (Ingvarsdóttir et al. 1999). Monitoring of these genes in copepods from different seasons exposed to different oxygen concentrations may provide closer insights.

Considering the metabolic reduction during diapause (Ingvarsdóttir et al. 1999), it is surprising that the major decrease in the lipid content and C/N ratio of deep layer CVs happened between August and November. The second generation CVs descending in October were smaller in size and thus could hold fewer lipids (Fig. 5A,D, Supporting Information Fig. S1) (Saumweber and Durbin 2006). In addition, they had to spend less time in diapause than the G<sub>1</sub> and thus possibly needed only smaller lipid reserves to survive. The difference in lipid content between G<sub>1</sub> and G<sub>2</sub> would explain the high variability in lipid levels of *C. finmarchicus* CVs sampled in November as well as the reduction in the deep layer lipid content and C/N ratio (Fig. 5C,D). Another explanation for the loss of lipids in these animals could be the higher metabolic rates associated with the warmer temperatures in Loch Etive compared to the North Atlantic (Ingvarsdóttir et al. 1999; Maps et al. 2014).

Rhythmic diel clock gene expression was present in the deep layer in May, but was lost with the physiological transition to diapause toward June (Fig. 8; Table 4). This suggests that the diel rhythmic output of the clock was actively “switched off” during diapause and that arrhythmicity was not just a consequence of the lack of light at depth, as also supported by the observation that in *C. finmarchicus* clock genes continue diel cycling in constant darkness (Häfker et al. 2017). As gene expression was determined from pooled individuals and because repeated measurements of the same individuals were not possible, the possibility that clocks remained rhythmic during diapause, but were desynchronized between individuals cannot be discounted. Although clock genes showed no diel cycling during diapause (Fig. 8; Table 4), several clock and clock-associated genes showed seasonal patterns of elevated expression during diapause from June to November (Fig. 7B) and a potential reason for this is discussed in the section “Mechanisms of diapause termination.”

### Emergence phase

Gene expression (Fig. 7) and increasing RNA yields (Fig. 6) indicate that the process of emergence from diapause started after the sampling in November and continued until the end of the study in March. The expression of genes associated with metabolic activity and developmental processes increased in

the S<sub>1</sub> and D<sub>1</sub> clusters, whereas the expression of genes related to diapause in the D<sub>3</sub> and D<sub>4</sub> clusters decreased. There was no increase in the expression of food-associated genes in the S<sub>2</sub> and D<sub>2</sub> clusters, likely because phytoplankton levels were still low in March.

Despite the upregulation of genes related to developmental processes, lipid levels stayed constant from November to March (Fig. 5D). A large proportion of storage lipids is used for gonad development (Rey-Rassat et al. 2002). This slow and energetically costly process starts several months before the ascent to the surface (Hirche 1996b; Jónasdóttir 1999; Niehoff et al. 2002). However, the major part of gonad maturation takes place during and after the molt to the adult stage (Tande 1982; Rey-Rassat et al. 2002), explaining why lipid content and C/N ratio of CV copepodids showed little change during emergence (Fig. 5C,D). Still, the constant deep layer lipid levels from November to March are surprising given the expected metabolic costs based on copepod size and ambient temperature (Ingvarsdóttir et al. 1999; Saumweber and Durbin 2006). Thus, it may be possible that copepods at depth fed heterotrophically to maintain lipid levels for maturation (Ohman and Runge 1994; Meyer-Harms et al. 1999) which would also explain why lipid content of deep layer CV copepodids increased from May to August despite low phytoplankton concentrations (Figs. 2E, 5D). The variance in the expression of individual genes stayed consistently low during the emergence phase (Supporting Information Fig. S2), suggesting that the copepods were all in the same physiological state. It appears that emergence was synchronized within the population, with all copepods resuming development and later ascending to surface waters at roughly the same time, although the G<sub>2</sub> entered diapause 3–4 months after the G<sub>1</sub> (Miller et al. 1991; Tittensor et al. 2003; Speirs et al. 2005; Baumgartner and Tarrant 2017).

Diel clock gene expression remained arrhythmic during emergence of the CV copepodids (Fig. 8; Table 4). However, it is noteworthy that in the shallow layer in March several clock genes showed (insignificant) tendencies of higher expression around sunset (Fig. 8). The ascent to surface waters typically takes place after the molt to the adult stage (Miller et al. 1991; Hirche 1996a), and the expression patterns suggest that the clock will be “switched on” soon after the molt. CV copepodids present in the shallow layer in November/January showed almost no clock gene cycling (exception: *vri* in November) although light levels should have been sufficient to entrain the clock (Table 4). The lack of clock cycling and similarities in seasonal clock gene expression patterns in the shallow and the deep layers from November to March (Figs. 7, 8) suggest that these shallow layer CV copepodids were not remnants of the active surface population, but rather diapausing copepods that had been advected to the surface. An active ascent in late autumn offers no ecological advantage and thus a passive transport from the deep layer seems most likely (Durbin et al. 1997) and is plausible as there was a partial exchange of Loch Etive deep water at this time. The

fact that the exposure to light at the surface did not “re-activate” clock gene cycling underpins the suggestion that the circadian clock is actively “switched off” in diapausing CV copepodids (Table 4).

### Mechanisms of diapause initiation

As highlighted in the introduction, the regulation and timing of diapause are still poorly understood and hence subject to debate (Baumgartner and Tarrant 2017). Currently, the most accepted hypothesis for the initiation of diapause is the “lipid accumulation window” (LAW) hypothesis (Rey-Rassat et al. 2002). The concept assumes a time window during which the copepods accumulate lipids toward a certain threshold representing the minimum amount needed to survive the time of diapause. In this context, the amount of accumulated lipids is also dependent on body size (Saumweber and Durbin 2006) and information about lipid status is possibly mediated via lipid-derived hormones (Irigoien 2004; Pond et al. 2012). The copepods that reach the “lipid-threshold” within the time window enter diapause while the others molt to adults and reproduce (Rey-Rassat et al. 2002) or may enter diapause with insufficient lipid reserves, leading to an early depletion and emergence (Maps et al. 2014). However, the continuous increase in lipid content in the deep layer CV copepodids from May to August argues against a specific lipid threshold triggering the physiological switch to diapause and the fact that  $G_1$  and  $G_2$  entered diapause with different amounts of lipids raises further doubts about the exclusive role of lipids in diapause initiation. Ecologically, the inability to accumulate sufficient lipid reserves indicates poor food conditions. If copepods mature and reproduce under these conditions, as suggested by the LAW hypothesis, their offspring would also have to face the same food limitation, potentially resulting in low survival rates (Søreide et al. 2010). In Loch Etive, this would affect the copepods in the shallow layer in November/January. However, gene expression data and clock rhythmicity imply that physiologically the animals had been, or were still, in diapause (Figs. 7, 8; Table 4). Further, the considerable amount of lipids found in shallow and deep layer copepods in November/January (Fig. 5D) argue against an early emergence due to insufficient lipid reserves.

An alternative hypothesis for the initiation of diapause assumes that the descent to diapause depth is related to low food concentrations (Hind et al. 2000). However, in Loch Etive, all copepods of the  $G_1$  experienced the same food conditions, not explaining why one fraction of the generation entered diapause while the others matured and produced a second generation.

In various insects and several copepods, the timing of diapause is controlled via photoperiod measurement by the circadian clock. In Loch Etive, the diel cycling of clock genes during the phase of activity and development shows the potential for photoperiod measurement in *C. finmarchicus* (Table 4). In insects and different life stages of calanoid and

cyclopoid copepods, diapause is mostly initiated in response to short photoperiods (Watson and Smallman 1971; Marcus 1982; Hairston and Kearns 1995; Meuti and Denlinger 2013; Salminen et al. 2015). In Loch Etive, the  $G_1$  entered diapause in June implying an extremely long critical photoperiod close to 18 h (Table 2). Although such long critical photoperiods have been reported (Hut et al. 2013), it seems unlikely that diapause initiation of *C. finmarchicus* in Loch Etive is based exclusively on photoperiod.

The triggers of diapause initiation in *C. finmarchicus* are still unknown, but probably involve the interaction of multiple internal and external factors (Miller et al. 1991; Johnson et al. 2008). Sufficient lipid reserves are crucial for surviving diapause, so that a critical minimum threshold of lipids is probably required before entering diapause (Rey-Rassat et al. 2002). However, photoperiod is a more reliable cue for the timing of the seasonal cycle that can trigger diapause in insects with high seasonal precision (Goto 2013; Meuti and Denlinger 2013). Hence, by the time a critical lipid threshold is reached, photoperiod might determine whether copepods enter diapause or mature to produce another generation. Further, temperature can modulate photoperiod-dependent diapause initiation in marine calanoid and freshwater cyclopoid copepods at the egg or the juvenile stage (Watson and Smallman 1971; Marcus 1982; Hairston and Kearns 1995). In spring/summer surface waters gradually warm and high temperatures might increase the likelihood of *C. finmarchicus* diapause initiation at a given photoperiod. However, it is also possible that the evasion of surface waters into deeper layers is a direct response to unfavorable temperature conditions (Kosobokova 1999; Niehoff and Hirche 2005).

Diapause triggers in *C. finmarchicus* might have been determined in an earlier life stage (Johnson et al. 2008). For example, in the freshwater cyclopoid copepod *Diacyclops navus* the photoperiod experienced during the CI stage determines if diapause is initiated in the CIV stage (Watson and Smallman 1971).

The existence of different clock gene alleles could explain the large differences in diapause timing between geographically distinct *C. finmarchicus* populations and also between generations within the same population (Durbin et al. 2000; Walkusz et al. 2009; Melle et al. 2014). Marcus (1984) found different critical photoperiods for the production of diapause eggs in populations of the same calanoid copepod species along the North American Atlantic coast and there are reports of different *tim*-alleles in *Drosophila* that modulate the diapause response to a given photoperiod (Sandrelli et al. 2007). The presence of different clock gene alleles among *C. finmarchicus* populations could lead to differences in the critical photoperiod, meaning that depending on the present alleles a given day length can initiate diapause in one population while copepods elsewhere mature and reproduce. The strong selective pressure on accurate diapause timing should lead to allele frequency differences among populations even if some genetic exchange exists between them. Different alleles within a population would

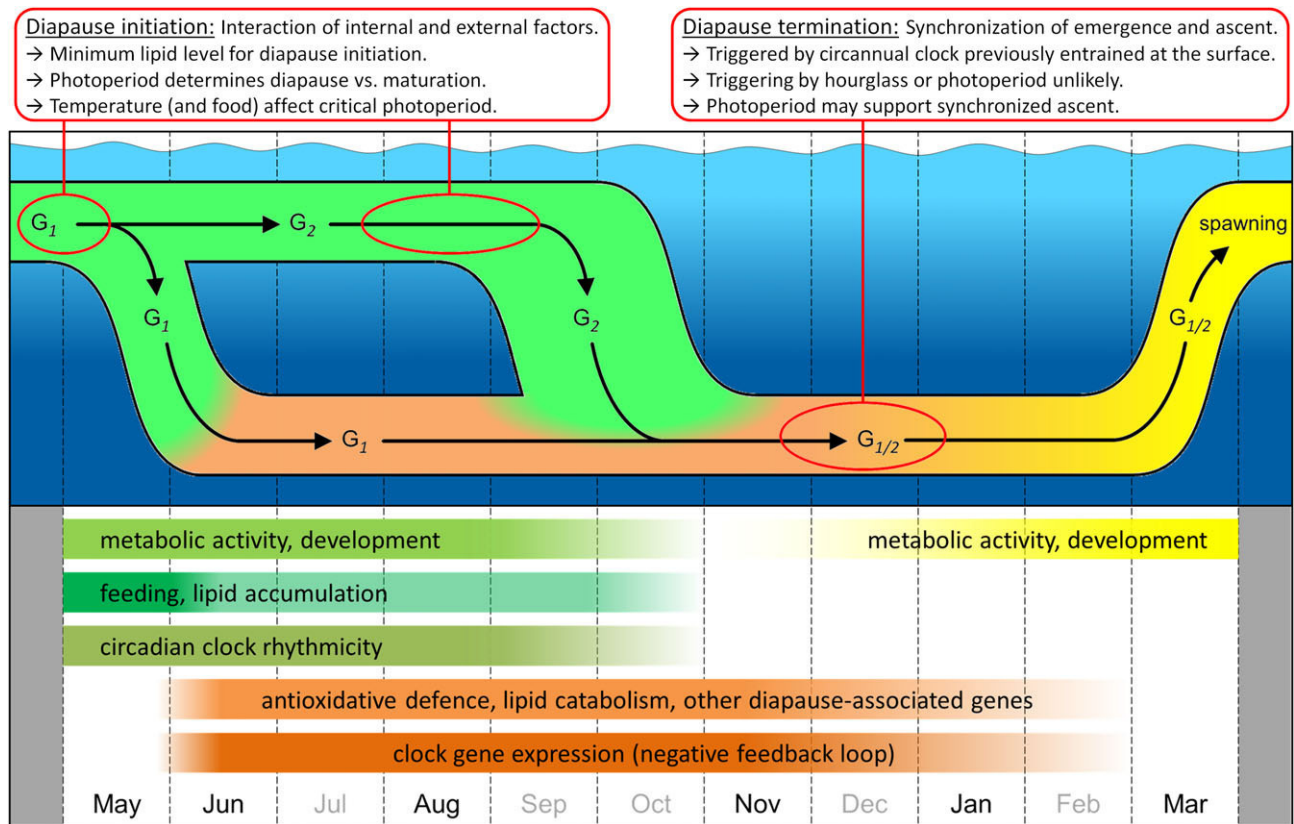


**Fig. 9.** *C. finmarchicus*' seasonal life cycle in Loch Etive. A schematic depiction of population dynamics, physiological changes, and potential diapause regulation mechanisms is shown. The spawning of the overwintering stock happened in April 2015 before the start of our study and is not shown. Colors indicate different life phases as well as the metabolic processes and gene groups characterizing the respective phases (green = activity/development, orange = diapause, yellow = emergence/ascent). Months printed gray were not sampled. Graphic was created with MS PowerPoint.

further explain why one fraction of a generation enters diapause while another fraction instead matures to produce a second generation (e.g., Durbin et al. 2000; Tarrant et al. 2008, this study). If both generations overwinter successfully, the respective alleles should be able to coexist within the population. Such genetically determined phenological diversity may be identified by comparing allele frequencies of genes involved in the clock and in light perception between different populations or generations of the same population. Generally, if diapause timing in *C. finmarchicus* or other ecological key species is to some extent determined genetically, this raises concerns about the adaptability to environmental changes like a shift in the seasonal timing of the phytoplankton bloom (Søreide et al. 2010; Leu et al. 2011).

### Mechanisms of diapause termination

In the open ocean, *C. finmarchicus* diapauses at depths between 400 m and 1000 m (Hirche 1996a; Heath et al. 2004) where seasonal changes of environmental parameters are minimal or absent. The potential lack of seasonal cues for triggering emergence has led to the proposal of an hourglass model based on the gradual depletion of wax esters (Miller et al. 1991; Campbell et al. 2004; Saumweber and Durbin

2006; Clark et al. 2012) mediated by lipid-derived hormones (Irigoiien 2004; Pond et al. 2012) or based on continuous slow development (Hind et al. 2000). However, our results from Loch Etive contradict this view. Lipid levels in diapausing *C. finmarchicus* CV copepodids were constant and little depleted during the phase of emergence from November to March and the  $G_1$  and  $G_2$  descended with different amounts of lipids and a delay of 3–4 months (Fig. 5D), making an hourglass-based synchronized emergence unlikely. As emergence was initiated well before the onset of the phytoplankton bloom, it is further unlikely that it was cued by particles sinking from the surface.

The repeatedly reported synchronized emergence in *C. finmarchicus* indicates a response to a reliable seasonal cue like photoperiod. However, PAR data reveal that light levels in the deep layer of Loch Etive were well below the copepods detection limit (Båtnes et al. 2013; Miljeteig et al. 2014). While a clock-based photoperiod measurement or hourglass timers therefore appear unsuitable for triggering emergence, the observed seasonal rhythmicity could be explained by a circannual clock that creates an endogenous rhythm with a period of ~ 365 days. Such endogenous annual rhythms have been described in many different

species, and although their molecular nature remains largely unresolved, it is agreed that photoperiod must play a crucial role in the entrainment of such long-range timing mechanisms (Randall et al. 1998; Goldman et al. 2004; Lincoln et al. 2006). For *C. finmarchicus*, the circadian clock-based photoperiodic entrainment of the circannual clock before the descent to diapause would ensure synchronized emergence as the  $G_1$  and the  $G_2$  experienced different photoperiods and thus their circannual rhythms should be synchronized in spite of them descending at different times. Circannual rhythms can run under constant conditions with astonishing precision over several years (Goldman et al. 2004) and they could also trigger emergence in the open ocean where light or other seasonal cues at diapause depth may be missing. Studies on other *Calanus* species showed that wild caught copepods kept under constant laboratory conditions for several months still emerged in synchrony with the field population, indicating that circannual timing exists in this genus (Conover 1965; Fulton 1973). Although handling stress during sampling may directly trigger emergence, a similar experimental approach could provide insights into potential circannual timing in *C. finmarchicus*. A putative circannual clock may share some components with the circadian clock, as several clock genes like *tim*, *per1/2*, and *cry2* were upregulated in diapause and their expression decreased after the onset of emergence (Fig. 7B), although the animals resided at constant darkness and diel rhythmicity ceased (Table 4).

Furthermore, it is noteworthy that the expression of the opsin gene *ops* was highest in the deep layer in November suggesting an increased sensitivity to light (Fig. 7B). Similarly, the expression of *cry1*, the gene considered responsible for the light entrainment of the circadian clock, increased during emergence. While copepods experienced constant darkness in the deep layer, Hill (2009) reported a gradual shoaling of *C. finmarchicus* diapause depth from January to March in Loch Etive, i.e., after the onset of emergence. Similar reports also exist for *Calanus* in the open ocean (Hirche 1997; Bandara et al. 2016). This was suggested to represent an ascent to depth where photoperiod measurement becomes possible thus aiding the synchronization of the emergence process within the population (Speirs et al. 2005). A rhythmic circadian clock may not be essential for this as photoperiod measurement could also be achieved without it (Emerson et al. 2009; Goto 2013). Although the exact regulatory mechanisms are still unclear, the combined insight from literature and our own results suggest that photoperiod—either directly or as an entrainment cue for a circannual clock—plays an important role in *C. finmarchicus* emergence from diapause.

## Conclusions

Focusing on the dominant CV copepodid stage, our results describe the seasonal life cycle of *C. finmarchicus*

consisting of a phase of activity and development in surface waters from May to October, diapause in deep waters from June to November, and a phase of emergence from November to March ending with the ascent to the surface (Fig. 9). Two generations of copepods were produced in the surface waters and descended to diapause in June and October, respectively. All phases of the seasonal cycle were characterized by distinct patterns of gene expression with several (e.g., *elov*, *fer*, *tim*, *ecr*, or *cyclB*) being potential proxies for the molecular determination of diapause status. While a circadian clock appears to regulate 24-h cycles in copepods actively developing in surface waters, diel clock gene cycling was absent in diapause and during emergence, although many clock genes showed highest expression during diapause. A general point to consider is that while light levels in Loch Etive are similar to the typical open ocean *Calanus* habitats due to high turbidity, pressure is lower and water temperatures are higher than would be expected at depth in the open ocean. This may have increased energy consumption in the copepods (Ingvarsdóttir et al. 1999; Heath et al. 2004), resulting in heterotrophic feeding and possibly an overall weaker diapause than in the open ocean. Our gene expression data resemble the few existing records from the open ocean, but it is clear that extensive field campaigns in open ocean habitats will be needed to compare the presented findings with other populations.

Seasonal patterns of physiology and gene expression in *C. finmarchicus* CV copepodids exclude lipid content and food as exclusive cues for the initiation or termination of diapause. Similarly, photoperiod alone cannot explain the observed seasonal diapause pattern. It is likely that the interactions of multiple external (photoperiod, temperature, and food concentration) and internal (circadian clock, lipid content, and hormones) factors determine whether the copepods enter diapause or mature to produce another generation. The synchronized emergence from diapause in spite of a lack of light at depth suggests a control mechanism involving an endogenous circannual clock entrained via photoperiod measurement before the descent to diapause depth (Fig. 9).

However, a mechanistic understanding of the factors controlling diapause remains elusive and can only now be gained from laboratory experiments (Baumgartner and Tarrant 2017). Considering our findings, combining the manipulation of external factors with the detailed monitoring of physiological and genetic parameters, could shed new light on the mechanisms of diapause regulation in *C. finmarchicus*.

## References

- Andersen, C. L., J. L. Jensen, and T. F. Ørntoft. 2004. Normalization of real-time quantitative reverse transcription-PCR data: A model-based variance estimation approach to identify genes suited for normalization, applied to bladder and

- colon cancer data sets. *Cancer Res.* **64**: 5245–5250. doi:[10.1158/0008-5472.CAN-04-0496](https://doi.org/10.1158/0008-5472.CAN-04-0496)
- Aruda, A. M., M. F. Baumgartner, A. M. Reitzel, and A. M. Tarrant. 2011. Heat shock protein expression during stress and diapause in the marine copepod *Calanus finmarchicus*. *J. Insect Physiol.* **57**: 665–675. doi:[10.1016/j.jinsphys.2011.03.007](https://doi.org/10.1016/j.jinsphys.2011.03.007)
- Aschoff, J. 1954. Zeitgeber der tierischen Tagesperiodik. *Naturwissenschaften* **41**: 49–56. doi:[10.1007/BF00634164](https://doi.org/10.1007/BF00634164)
- Båmstedt, U. 1988. Interspecific, seasonal and diel variations in zooplankton trypsin and amylase activities in Kosterfjorden, western Sweden. *Mar. Ecol. Prog. Ser.* **44**: 15–24. doi:[10.3354/meps044015](https://doi.org/10.3354/meps044015)
- Bandara, K., Ø. Varpe, J. E. Søreide, J. Wallenschus, J. Berge, and K. Eiane. 2016. Seasonal vertical strategies in a high-Arctic coastal zooplankton community. *Mar. Ecol. Prog. Ser.* **555**: 49–64. doi:[10.3354/meps11831](https://doi.org/10.3354/meps11831)
- Båtnes, A. S., C. Miljeteig, J. Berge, M. Greenacre, and G. Johnsen. 2013. Quantifying the light sensitivity of *Calanus* spp. during the polar night: Potential for orchestrated migrations conducted by ambient light from the sun, moon, or aurora borealis? *Polar Biol.* **38**: 51–65. doi:[10.1007/s00300-013-1415-4](https://doi.org/10.1007/s00300-013-1415-4)
- Baumgartner, M. F., and A. M. Tarrant. 2017. The physiology and ecology of diapause in marine copepods. *Ann. Rev. Mar. Sci.* **9**: 387–411. doi:[10.1146/annurev-marine-010816-060505](https://doi.org/10.1146/annurev-marine-010816-060505)
- Berge, J., and others. 2009. Diel vertical migration of Arctic zooplankton during the polar night. *Biol. Lett.* **5**: 69–72. doi:[10.1098/rsbl.2008.0484](https://doi.org/10.1098/rsbl.2008.0484)
- Bingham, C., B. Arbogast, G. C. Guillaume, J. K. Lee, and F. Halberg. 1982. Inferential statistical methods for estimating and comparing cosinor parameters. *Chronobiologia* **9**: 397–439.
- Brierley, A. S. 2014. Diel vertical migration. *Curr. Biol.* **24**: R1074–R1076. doi:[10.1016/j.cub.2014.08.054](https://doi.org/10.1016/j.cub.2014.08.054)
- Brierley, A. S., R. A. Saunders, D. G. Bone, E. J. Murphy, P. Enderlein, S. G. Conti, and D. A. Demer. 2006. Use of moored acoustic instruments to measure short-term variability in abundance of Antarctic krill. *Limnol. Oceanogr.* **51**: 18–29. doi:[10.4319/lom.2006.4.18](https://doi.org/10.4319/lom.2006.4.18)
- Bünning, E. 1960. Circadian rhythms and the time measurement in photoperiodism. *Cold Spring Harb. Symp. Quant. Biol.* **25**: 249–256. doi:[10.1101/SQB.1960.025.01.026](https://doi.org/10.1101/SQB.1960.025.01.026)
- Campbell, R. W., P. Boutillier, and J. F. Dower. 2004. Ecophysiology of overwintering in the copepod *Neocalanus plumchrus*: Changes in lipid and protein contents over a seasonal cycle. *Mar. Ecol. Prog. Ser.* **280**: 211–226. doi:[10.3354/meps280211](https://doi.org/10.3354/meps280211)
- Casteels, M., M. Sniekers, P. Fraccascia, G. P. Mannaerts, and P. P. Van Veldhoven. 2007. The role of 2-hydroxyacyl-CoA lyase, a thiamin pyrophosphate-dependent enzyme, in the peroxisomal metabolism of 3-methyl-branched fatty acids and 2-hydroxy straight-chain fatty acids. *Biochem. Soc. Trans.* **35**: 876–880. doi:[10.1042/BST0350876](https://doi.org/10.1042/BST0350876)
- Ceriani, M. F., J. B. Hogenesch, M. Yanovsky, S. Panda, M. Straume, and S. A. Kay. 2002. Genome-wide expression analysis in *Drosophila* reveals genes controlling circadian behavior. *J. Neurosci.* **22**: 9305–9319. doi:[10.1523/JNEUROSCI.22-21-09305.2002](https://doi.org/10.1523/JNEUROSCI.22-21-09305.2002)
- Chandel, N. S., D. S. McClintock, C. E. Feliciano, T. M. Wood, J. A. Melendez, A. M. Rodriguez, and P. T. Schumacker. 2000. Reactive oxygen species generated at mitochondrial complex III stabilize hypoxia-inducible factor-1 $\alpha$  during hypoxia a mechanism of O<sub>2</sub> sensing. *J. Biol. Chem.* **275**: 25130–25138. doi:[10.1074/jbc.M001914200](https://doi.org/10.1074/jbc.M001914200)
- Christie, A. E., T. M. Fontanilla, K. T. Nesbit, and P. H. Lenz. 2013a. Prediction of the protein components of a putative *Calanus finmarchicus* (Crustacea, Copepoda) circadian signaling system using a de novo assembled transcriptome. *Comp. Biochem. Physiol. Part D Genomics Proteomics* **8**: 165–193. doi:[10.1016/j.cbd.2013.04.002](https://doi.org/10.1016/j.cbd.2013.04.002)
- Christie, A. E., V. Roncalli, P. B. Lona, M. D. McCoole, B. L. King, A. Bucklin, D. K. Hartline, and P. H. Lenz. 2013b. *In silico* characterization of the insect diapause-associated protein couch potato (CPO) in *Calanus finmarchicus* (Crustacea: Copepoda). *Comp. Biochem. Physiol. Part D Genomics Proteomics* **8**: 45–57. doi:[10.1016/j.cbd.2012.11.002](https://doi.org/10.1016/j.cbd.2012.11.002)
- Clark, K. A. J., A. S. Brierley, and D. W. Pond. 2012. Composition of wax esters is linked to diapause behavior of *Calanus finmarchicus* in a sea loch environment. *Limnol. Oceanogr.* **57**: 65–75. doi:[10.4319/lo.2012.57.1.0065](https://doi.org/10.4319/lo.2012.57.1.0065)
- Clark, K. A. J., A. S. Brierley, D. W. Pond, and V. J. Smith. 2013. Changes in seasonal expression patterns of ecdysone receptor, retinoid X receptor and an A-type allatostatin in the copepod, *Calanus finmarchicus*, in a sea loch environment: An investigation of possible mediators of diapause. *Gen. Comp. Endocrinol.* **189**: 66–73. doi:[10.1016/j.ygcen.2013.04.002](https://doi.org/10.1016/j.ygcen.2013.04.002)
- Cohen, J. H., and R. B. Forward Jr. 2005. Diel vertical migration of the marine copepod *Calanopia americana*. II. Proximate role of exogenous light cues and endogenous rhythms. *Mar. Biol.* **147**: 399–410. doi:[10.1007/s00227-005-1570-4](https://doi.org/10.1007/s00227-005-1570-4)
- Cohen, J. H., and others. 2015. Is ambient light during the high Arctic polar night sufficient to act as a visual cue for zooplankton? *PLoS One* **10**: e0126247. doi:[10.1371/journal.pone.0126247](https://doi.org/10.1371/journal.pone.0126247)
- Conover, R. J. 1965. Notes on the molting cycle, development of sexual characters and sex ratio in *Calanus hyperboreus*. *Crustaceana* **8**: 308–320. doi:[10.1163/156854065X00497](https://doi.org/10.1163/156854065X00497)
- Conover, R. J. 1988. Comparative life histories in the genera *Calanus* and *Neocalanus* in high latitudes of the northern hemisphere. *Hydrobiologia* **167–168**: 127–142. doi:[10.1007/BF00026299](https://doi.org/10.1007/BF00026299)
- Cottier, F. R., G. A. Tarling, A. Wold, and S. Falk-Petersen. 2006. Unsynchronized and synchronized vertical migration of zooplankton in a high arctic fjord. *Limnol. Oceanogr.* **51**: 2586–2599. doi:[10.4319/lo.2006.51.6.2586](https://doi.org/10.4319/lo.2006.51.6.2586)

- Deines, K. L. 1999. Backscatter estimation using Broadband acoustic Doppler current profilers, p. 249–253. *In* Proceedings of the IEEE Sixth Working Conference on Current Measurement. doi:10.1109/CCM.1999.755249
- Durbin, E. G., J. A. Runge, R. G. Campbell, P. R. Garrahan, M. C. Casas, and S. Plourde. 1997. Late fall-early winter recruitment of *Calanus finmarchicus* on Georges Bank. *Mar. Ecol. Prog. Ser.* **151**: 103–114. doi:10.3354/meps151103
- Durbin, E. G., P. R. Garrahan, and M. C. Casas. 2000. Abundance and distribution of *Calanus finmarchicus* on the Georges Bank during 1995 and 1996. *ICES J. Mar. Sci. J. Cons.* **57**: 1664–1685. doi:10.1006/jmsc.2000.0974
- Edwards, A., and D. J. Edelsten. 1977. Deep water renewal of Loch Etive: A three basin Scottish fjord. *Estuar. Coast. Mar. Sci.* **5**: 575–595. doi:10.1016/0302-3524(77)90085-8
- Einsle, U. 1964. Larvalentwicklung von Cyclopiden und Photoperiodik. *Naturwissenschaften* **51**: 345–345. doi:10.1007/BF00625096
- Emerson, K. J., S. J. Dake, W. E. Bradshaw, and C. M. Holzapfel. 2009. Evolution of photoperiodic time measurement is independent of the circadian clock in the pitcher-plant mosquito, *Wyeomyia smithii*. *J. Comp. Physiol. A* **195**: 385–391. doi:10.1007/s00359-009-0416-9
- Enright, J. T., and W. M. Hamner. 1967. Vertical diurnal migration and endogenous rhythmicity. *Science* **157**: 937–941. doi:10.1126/science.157.3791.937
- Falk-Petersen, S., P. Mayzaud, G. Kattner, and J. R. Sargent. 2009. Lipids and life strategy of Arctic *Calanus*. *Mar. Biol. Res.* **5**: 18–39. doi:10.1080/17451000802512267
- Folch, J., M. Lees, and G. H. S. Stanley. 1957. A simple method for the isolation and purification of total lipides from animal tissues. *J. Biol. Chem.* **226**: 497–509.
- Freese, D., B. Niehoff, J. E. Søreide, and F. J. Sartoris. 2015. Seasonal patterns in extracellular ion concentrations and pH of the Arctic copepod *Calanus glacialis*. *Limnol. Oceanogr.* **60**: 2121–2129. doi:10.1002/lno.10158
- Freese, D., J. E. Søreide, M. Graeve, and B. Niehoff. 2017. A year-round study on metabolic enzymes and body composition of the Arctic copepod *Calanus glacialis*: Implications for the timing and intensity of diapause. *Mar. Biol.* **164**: 3. doi:10.1007/s00227-016-3036-2
- Fu, W., and others. 2013. Exploring valid reference genes for quantitative real-time PCR analysis in *Plutella xylostella* (Lepidoptera: Plutellidae). *Int. J. Biol. Sci.* **9**: 792–802. doi:10.7150/ijbs.5862
- Fulton, J. 1973. Some aspects of the life history of *Calanus plumchrus* in the Strait of Georgia. *J. Fish. Res. Board Can.* **30**: 811–815. doi:10.1139/f73-136
- Goldman, B., E. Gwinner, F. J. Karsch, D. Saunders, I. Zucker, and G. F. Gall. 2004. Circannual rhythms and photoperiodism, p. 107–142. *In* J. C. Dunlap, J. J. Loros, and P. J. DeCoursey [eds.], *Chronobiology: Biological timekeeping*. Sinauer.
- Goto, S. G. 2013. Roles of circadian clock genes in insect photoperiodism. *Entomol. Sci.* **16**: 1–16. doi:10.1111/ens.12000
- Grigg, H., and S. J. Bardwell. 1982. Seasonal observations on moulting and maturation in Stage V copepodites of *Calanus finmarchicus* from the Firth of Clyde. *J. Mar. Biol. Assoc. UK* **62**: 315–327. doi:10.1017/S0025315400057301
- Häfker, N. S., B. Meyer, K. S. Last, D. W. Pond, L. Hüppe, and M. Teschke. 2017. Circadian clock involvement in zooplankton diel vertical migration. *Curr. Biol.* **27**: 2194–2201. e3. doi:10.1016/j.cub.2017.06.025
- Hahn, D. A., and D. L. Denlinger. 2011. Energetics of insect diapause. *Annu. Rev. Entomol.* **56**: 103–121. doi:10.1146/annurev-ento-112408-085436
- Hairston, N. G., and C. M. Kearns. 1995. The interaction of photoperiod and temperature in diapause timing: A copepod example. *Biol. Bull.* **189**: 42–48. doi:10.2307/1542200
- Hallberg, E., and H.-J. Hirche. 1980. Differentiation of mid-gut in adults and over-wintering copepodids of *Calanus finmarchicus* (Gunnerus) and *C. helgolandicus* Claus. *J. Exp. Mar. Bio. Ecol.* **48**: 283–295. doi:10.1016/0022-0981(80)90083-0
- Hansen, B. H., D. Altin, K. M. Hessen, U. Dahl, M. Breitholtz, T. Nordtug, and A. J. Olsen. 2008. Expression of ecdysteroids and cytochrome P450 enzymes during lipid turnover and reproduction in *Calanus finmarchicus* (Crustacea: Copepoda). *Gen. Comp. Endocrinol.* **158**: 115–121. doi:10.1016/j.ygcen.2008.05.013
- Harris, R. P., and others. 2000. Feeding, growth, and reproduction in the genus *Calanus*. *ICES J. Mar. Sci.* **57**: 1708–1726. doi:10.1006/jmsc.2000.0959
- Hassett, R. P. 2006. Physiological characteristics of lipid-rich" fat" and lipid-poor" thin" morphotypes of individual *Calanus finmarchicus* C5 copepodites in nearshore Gulf of Maine. *Limnol. Oceanogr.* **51**: 997–1003. doi:10.4319/lo.2006.51.2.0997
- Hassett, R. P., P. H. Lenz, and D. W. Towle. 2010. Gene expression and biochemical studies of the marine copepod *Calanus finmarchicus*. *MDI Biol. Lab. Bull.* **49**: 115–117.
- He, H.-M., Z.-H. Xian, F. Huang, X.-P. Liu, and F.-S. Xue. 2009. Photoperiodism of diapause induction in *Thyrsia penangae* (Lepidoptera: Zygaenidae). *J. Insect Physiol.* **55**: 1003–1008. doi:10.1016/j.jinsphys.2009.07.004
- Head, E. J. H., and L. R. Harris. 1985. Physiological and biochemical changes in *Calanus hyperboreus* from Jones Sound NWT during the transition from summer feeding to over-wintering condition. *Polar Biol.* **4**: 99–106. doi:10.1007/BF00442907
- Heath, M. R., and others. 2004. Comparative ecology of over-wintering *Calanus finmarchicus* in the northern North Atlantic, and implications for life-cycle patterns. *ICES J. Mar. Sci.* **61**: 698–708. doi:10.1016/j.icesjms.2004.03.013
- Helaouët, P., and G. Beaugrand. 2007. Macroecology of *Calanus finmarchicus* and *C. helgolandicus* in the North Atlantic

- Ocean and adjacent seas. *Mar. Ecol. Prog. Ser.* **345**: 147–165. doi:[10.3354/meps06775](https://doi.org/10.3354/meps06775)
- Hill, K. A. 2009. Changes in gene expression, lipid class and fatty acid composition associated with diapause in the marine copepod *Calanus finmarchicus* from Loch Etive, Scotland. Ph.D. thesis. Univ. of St Andrews.
- Hind, A., W. S. C. Gurney, M. Heath, and A. D. Bryant. 2000. Overwintering strategies in *Calanus finmarchicus*. *Mar. Ecol. Prog. Ser.* **193**: 95–107. doi:[10.3354/meps193095](https://doi.org/10.3354/meps193095)
- Hirche, H.-J. 1996a. Diapause in the marine copepod, *Calanus finmarchicus*—a review. *Ophelia* **44**: 129–143. doi:[10.1080/00785326.1995.10429843](https://doi.org/10.1080/00785326.1995.10429843)
- Hirche, H.-J. 1996b. The reproductive biology of the marine copepod, *Calanus finmarchicus*—a review. *Ophelia* **44**: 111–128. doi:[10.1080/00785326.1995.10429842](https://doi.org/10.1080/00785326.1995.10429842)
- Hirche, H.-J. 1997. Life cycle of the copepod *Calanus hyperboreus* in the Greenland Sea. *Mar. Biol.* **128**: 607–618. doi:[10.1007/s002270050127](https://doi.org/10.1007/s002270050127)
- Hut, R. A., S. Paolucci, R. Dor, C. P. Kyriacou, and S. Daan. 2013. Latitudinal clines: An evolutionary view on biological rhythms. *Proc. R. Soc. B Biol. Sci.* **280**: 20130433. doi:[10.1098/rspb.2013.0433](https://doi.org/10.1098/rspb.2013.0433)
- Ingvarsdóttir, A., D. F. Houlihan, M. R. Heath, and S. J. Hay. 1999. Seasonal changes in respiration rates of copepodite stage V *Calanus finmarchicus* (Gunnerus). *Fish. Oceanogr.* **8**: 73–83. doi:[10.1046/j.1365-2419.1999.00002.x](https://doi.org/10.1046/j.1365-2419.1999.00002.x)
- Irigoién, X. 2004. Some ideas about the role of lipids in the life cycle of *Calanus finmarchicus*. *J. Plankton Res.* **26**: 259–263. doi:[10.1093/plankt/fbh030](https://doi.org/10.1093/plankt/fbh030)
- Irigoién, X., D. V. P. Conway, and R. P. Harris. 2004. Flexible diel vertical migration behaviour of zooplankton in the Irish Sea. *Mar. Ecol. Prog. Ser.* **267**: 85–97. doi:[10.3354/meps267085](https://doi.org/10.3354/meps267085)
- Ji, R. 2011. *Calanus finmarchicus* diapause initiation: New view from traditional life history-based model. *Mar. Ecol. Prog. Ser.* **440**: 105–114. doi:[10.3354/meps09342](https://doi.org/10.3354/meps09342)
- Johnson, C. L., A. W. Leising, J. A. Runge, E. J. Head, P. Pepin, S. Plourde, and E. G. Durbin. 2008. Characteristics of *Calanus finmarchicus* dormancy patterns in the Northwest Atlantic. *ICES J. Mar. Sci. J. Cons.* **65**: 339–350. doi:[10.1093/icesjms/fsm171](https://doi.org/10.1093/icesjms/fsm171)
- Jónasdóttir, S. H. 1999. Lipid content of *Calanus finmarchicus* during overwintering in the Faroe–Shetland Channel. *Fish. Oceanogr.* **8**: 61–72. doi:[10.1046/j.1365-2419.1999.00003.x](https://doi.org/10.1046/j.1365-2419.1999.00003.x)
- Kosobokova, K. N. 1999. The reproductive cycle and life history of the Arctic copepod *Calanus glacialis* in the White Sea. *Polar Biol.* **22**: 254–263. doi:[10.1007/s003000050418](https://doi.org/10.1007/s003000050418)
- Kwasniewski, S., H. Hop, S. Falk-Petersen, and G. Pedersen. 2003. Distribution of *Calanus* species in Kongsfjorden, a glacial fjord in Svalbard. *J. Plankton Res.* **25**: 1–20. doi:[10.1093/plankt/25.1.1](https://doi.org/10.1093/plankt/25.1.1)
- Lass, S., and P. Spaak. 2003. Chemically induced anti-predator defences in plankton: A review. *Hydrobiologia* **491**: 221–239. doi:[10.1023/A:1024487804497](https://doi.org/10.1023/A:1024487804497)
- Last, K. S., L. Hobbs, J. Berge, A. S. Brierley, and F. Cottier. 2016. Moonlight drives ocean-scale mass vertical migration of zooplankton during the Arctic winter. *Curr. Biol.* **26**: 1–8. doi:[10.1016/j.cub.2015.11.038](https://doi.org/10.1016/j.cub.2015.11.038)
- Lenz, P. H., V. Roncalli, R. P. Hassett, L.-S. Wu, M. C. Cieslak, D. K. Hartline, and A. E. Christie. 2014. *De novo* assembly of a transcriptome for *Calanus finmarchicus* (Crustacea, Copepoda)—the dominant zooplankton of the North Atlantic Ocean. *PLoS One* **9**: e88589. doi:[10.1371/journal.pone.0088589](https://doi.org/10.1371/journal.pone.0088589)
- Leu, E., J. E. Søreide, D. O. Hessen, S. Falk-Petersen, and J. Berge. 2011. Consequences of changing sea-ice cover for primary and secondary producers in the European Arctic shelf seas: Timing, quantity, and quality. *Prog. Oceanogr.* **90**: 18–32. doi:[10.1016/j.pocean.2011.02.004](https://doi.org/10.1016/j.pocean.2011.02.004)
- Lincoln, G. A., I. J. Clarke, R. A. Hut, and D. G. Hazlerigg. 2006. Characterizing a mammalian circannual pacemaker. *Science* **314**: 1941–1944. doi:[10.1126/science.1132009](https://doi.org/10.1126/science.1132009)
- Livak, K. J., and T. D. Schmittgen. 2001. Analysis of relative gene expression data using real-time quantitative PCR and the 2- $\Delta\Delta$ CT method. *Methods* **25**: 402–408. doi:[10.1006/meth.2001.1262](https://doi.org/10.1006/meth.2001.1262)
- Mackey, S. R. 2007. Biological rhythms workshop IA: Molecular basis of rhythms generation. *Cold Spring Harb Symp. Quant. Biol.* **72**: 7–19. doi:[10.1101/sqb.2007.72.060](https://doi.org/10.1101/sqb.2007.72.060)
- Maps, F., J. A. Runge, A. Leising, A. J. Pershing, N. R. Record, S. Plourde, and J. J. Pierson. 2011. Modelling the timing and duration of dormancy in populations of *Calanus finmarchicus* from the Northwest Atlantic shelf. *J. Plankton Res.* **34**: 36–54. doi:[10.1093/plankt/fbr088](https://doi.org/10.1093/plankt/fbr088)
- Maps, F., N. R. Record, and A. J. Pershing. 2014. A metabolic approach to dormancy in pelagic copepods helps explaining inter- and intra-specific variability in life-history strategies. *J. Plankton Res.* **36**: 18–30. doi:[10.1093/plankt/fbt100](https://doi.org/10.1093/plankt/fbt100)
- Marcus, N. H. 1982. Photoperiodic and temperature regulation of diapause in *Labidocera aestiva* (Copepoda: Calanoida). *Biol. Bull.* **162**: 45–52. doi:[10.2307/1540969](https://doi.org/10.2307/1540969)
- Marcus, N. H. 1984. Variation in the diapause response of *Labidocera aestiva* (copepoda: calanoida) from different latitudes and its importance in the evolutionary process. *Biol. Bull.* **166**: 127–139. doi:[10.2307/1541436](https://doi.org/10.2307/1541436)
- Marshall, S. M., and A. P. Orr. 1955. The biology of a marine copepod, *Calanus finmarchicus* (Gunnerus). Oliver and Boyd.
- Mauchline, J. 1987. Zooplankton in the Oban area and especially in Upper Loch Etive. *Scott. Mar. Biol. Assoc. Intern. Rep.* **144**: 1–91.
- Melle, W., and others. 2014. The North Atlantic Ocean as habitat for *Calanus finmarchicus*: Environmental factors and life history traits. *Prog. Oceanogr.* **129**: 244–284. doi:[10.1016/j.pocean.2014.04.026](https://doi.org/10.1016/j.pocean.2014.04.026)
- Merlin, C., R. J. Gegear, and S. M. Reppert. 2009. Antennal circadian clocks coordinate sun compass orientation in migratory monarch butterflies. *Science* **325**: 1700–1704. doi:[10.1126/science.1176221](https://doi.org/10.1126/science.1176221)

- Meuti, M. E., and D. L. Denlinger. 2013. Evolutionary links between circadian clocks and photoperiodic diapause in insects. *Integr. Comp. Biol.* **53**: 131–143. doi:[10.1093/icb/ict023](https://doi.org/10.1093/icb/ict023)
- Meyer, B., R. Saborowski, A. Atkinson, F. Buchholz, and U. Bathmann. 2002. Seasonal differences in citrate synthase and digestive enzyme activity in larval and postlarval antarctic krill, *Euphausia superba*. *Mar. Biol.* **141**: 855–862. doi:[10.1007/s00227-002-0877-7](https://doi.org/10.1007/s00227-002-0877-7)
- Meyer, B., and others. 2010. Seasonal variation in body composition, metabolic activity, feeding, and growth of adult krill *Euphausia superba* in the Lazarev Sea. *Mar. Ecol. Prog. Ser.* **398**: 1–18. doi:[10.3354/meps08371](https://doi.org/10.3354/meps08371)
- Meyer-Harms, B., X. Irigoien, R. Head, and R. Harris. 1999. Selective feeding on natural phytoplankton by *Calanus finmarchicus* before, during, and after the 1997 spring bloom in the Norwegian Sea. *Limnol. Oceanogr.* **44**: 154–165. doi:[10.4319/lo.1999.44.1.0154](https://doi.org/10.4319/lo.1999.44.1.0154)
- Miljeteig, C., A. J. Olsen, A. S. Båtnes, D. Altin, T. Nordtug, M. O. Alver, J. D. M. Speed, and B. M. Jenssen. 2014. Sex and life stage dependent phototactic response of the marine copepod *Calanus finmarchicus* (Copepoda: Calanoida). *J. Exp. Mar. Bio. Ecol.* **451**: 16–24. doi:[10.1016/j.jembe.2013.10.032](https://doi.org/10.1016/j.jembe.2013.10.032)
- Miller, C. B., T. J. Cowles, P. H. Wiebe, N. J. Copley, and H. Grigg. 1991. Phenology in *Calanus finmarchicus*; hypotheses about control mechanisms. *Mar. Ecol. Prog. Ser.* **72**: 79–91. doi:[10.3354/meps072079](https://doi.org/10.3354/meps072079)
- Morata, N., and J. E. Søreide. 2013. Effect of light and food on the metabolism of the Arctic copepod *Calanus glacialis*. *Polar Biol.* **38**: 67–73. doi:[10.1007/s00300-013-1417-2](https://doi.org/10.1007/s00300-013-1417-2)
- Neuwirth, E.. 2014. RColorBrewer: ColorBrewer Palettes.
- Nichols, J. H., and A. B. Thompson. 1991. Mesh selection of copepodite and nauplius stages of four calanoid copepod species. *J. Plankton Res.* **13**: 661–671. doi:[10.1093/plankt/13.3.661](https://doi.org/10.1093/plankt/13.3.661)
- Niehoff, B., U. Klenke, H. Hirche, X. Irigoien, R. Head, and R. Harris. 1999. A high frequency time series at Weathership M, Norwegian Sea, during the 1997 spring bloom: The reproductive biology of *Calanus finmarchicus*. *Mar. Ecol. Prog. Ser.* **176**: 81–92. doi:[10.3354/meps176081](https://doi.org/10.3354/meps176081)
- Niehoff, B., S. Madsen, B. Hansen, and T. Nielsen. 2002. Reproductive cycles of three dominant *Calanus* species in Disko Bay, West Greenland. *Mar. Biol.* **140**: 567–576. doi:[10.1007/s00227-001-0731-3](https://doi.org/10.1007/s00227-001-0731-3)
- Niehoff, B., and H.-J. Hirche. 2005. Reproduction of *Calanus glacialis* in the Lurefjord (western Norway): Indication for temperature-induced female dormancy. *Mar. Ecol. Prog. Ser.* **285**: 107–115. doi:[10.3354/meps285107](https://doi.org/10.3354/meps285107)
- Nørgaard-Pedersen, N., W. E. N. Austin, J. A. Howe, and T. Shimmiel. 2006. The Holocene record of Loch Etive, western Scotland: Influence of catchment and relative sea level changes. *Mar. Geol.* **228**: 55–71. doi:[10.1016/j.margeo.2006.01.001](https://doi.org/10.1016/j.margeo.2006.01.001)
- Ogle, D. H. 2017. FSA: Fisheries stock analysis. R package version 0.8.17.
- Ohman, M. D., and J. A. Runge. 1994. Sustained fecundity when phytoplankton resources are in short supply: Omnivory by *Calanus finmarchicus* in the Gulf of St. Lawrence. *Limnol. Oceanogr.* **39**: 21–36. doi:[10.4319/lo.1994.39.1.0021](https://doi.org/10.4319/lo.1994.39.1.0021)
- Oster, H., E. Maronde, and U. Albrecht. 2002. The circadian clock as a molecular calendar. *Chronobiol. Int.* **19**: 507–516. doi:[10.1081/CBI-120004210](https://doi.org/10.1081/CBI-120004210)
- Panda, S., and others. 2002. Coordinated transcription of key pathways in the mouse by the circadian clock. *Cell* **109**: 307–320. doi:[10.1016/S0092-8674\(02\)00722-5](https://doi.org/10.1016/S0092-8674(02)00722-5)
- Pierson, J. J., H. Batchelder, W. Saumweber, A. Leising, and J. Runge. 2013. The impact of increasing temperatures on dormancy duration in *Calanus finmarchicus*. *J. Plankton Res.* **35**: 504–512. doi:[10.1093/plankt/fbt022](https://doi.org/10.1093/plankt/fbt022)
- Pittendrigh, C. S. 1960. Circadian rhythms and the circadian organization of living systems. *Cold Spring Harb. Symp. Quant. Biol.* **25**: 159–184. doi:[10.1101/SQB.1960.025.01.015](https://doi.org/10.1101/SQB.1960.025.01.015)
- Plourde, S., P. Joly, J. A. Runge, B. Zakardjian, and J. J. Dodson. 2001. Life cycle of *Calanus finmarchicus* in the lower St. Lawrence Estuary: The imprint of circulation and late timing of the spring phytoplankton bloom. *Can. J. Fish. Aquat. Sci.* **58**: 647–658. doi:[10.1139/f01-006](https://doi.org/10.1139/f01-006)
- Poelchau, M. F., J. A. Reynolds, C. G. Elsik, D. L. Denlinger, and P. A. Armbruster. 2013. Deep sequencing reveals complex mechanisms of diapause preparation in the invasive mosquito, *Aedes albopictus*. *Proc. R. Soc. Lond. B Biol. Sci.* **280**: 20130143. doi:[10.1098/rspb.2013.0143](https://doi.org/10.1098/rspb.2013.0143)
- Pond, D. W., G. A. Tarling, P. Ward, and D. J. Mayor. 2012. Wax ester composition influences the diapause patterns in the copepod *Calanoides acutus*. *Deep-Sea Res. Part II Top. Stud. Oceanogr.* **59**: 93–104. doi:[10.1016/j.dsr2.2011.05.009](https://doi.org/10.1016/j.dsr2.2011.05.009)
- Prokopchuk, I., and E. Sentyabov. 2006. Diets of herring, mackerel, and blue whiting in the Norwegian Sea in relation to *Calanus finmarchicus* distribution and temperature conditions. *ICES J. Mar. Sci. J. Cons.* **63**: 117–127. doi:[10.1016/j.icesjms.2005.08.005](https://doi.org/10.1016/j.icesjms.2005.08.005)
- R Development Core Team. 2013. R: A language and environment for statistical computing.
- Randall, C. F., N. R. Bromage, J. Duston, and J. Symes. 1998. Photoperiod-induced phase-shifts of the endogenous clock controlling reproduction in the rainbow trout: A circannual phase–response curve. *J. Reprod. Fertil.* **112**: 399–405. doi:[10.1530/jrf.0.1120399](https://doi.org/10.1530/jrf.0.1120399)
- Reddy, A. B., and G. Rey. 2014. Metabolic and nontranscriptional circadian clocks: Eukaryotes. *Annu. Rev. Biochem.* **83**: 165–189. doi:[10.1146/annurev-biochem-060713-035623](https://doi.org/10.1146/annurev-biochem-060713-035623)
- Rey-Rassat, C., X. Irigoien, R. Harris, and F. Carlotti. 2002. Energetic cost of gonad development in *Calanus*

- finmarchicus* and *C. helgolandicus*. Mar. Ecol. Prog. Ser. **238**: 301–306. doi:[10.3354/meps238301](https://doi.org/10.3354/meps238301)
- Richier, B., C. Michard-Vanhée, A. Lamouroux, C. Papin, and F. Rouyer. 2008. The clockwork orange *Drosophila* protein functions as both an activator and a repressor of clock gene expression. J. Biol. Rhythms **23**: 103–116. doi:[10.1177/0748730407313817](https://doi.org/10.1177/0748730407313817)
- Runge, J. A. 1988. Should we expect a relationship between primary production and fisheries? The role of copepod dynamics as a filter of trophic variability. Hydrobiologia **167/168**: 61–71. doi:[10.1007/BF00026294](https://doi.org/10.1007/BF00026294)
- Sakamoto, T., O. Uryu, and K. Tomioka. 2009. The clock gene *period* plays an essential role in photoperiodic control of nymphal development in the cricket *Modicogryllus siamensis*. J. Biol. Rhythms **24**: 379–390. doi:[10.1177/0748730409341523](https://doi.org/10.1177/0748730409341523)
- Salminen, T. S., L. Vesala, A. Laiho, M. Merisalo, A. Hoikkala, and M. Kankare. 2015. Seasonal gene expression kinetics between diapause phases in *Drosophila virilis* group species and overwintering differences between diapausing and non-diapausing females. Sci. Rep. **5**: 11197. doi:[10.1038/srep11197](https://doi.org/10.1038/srep11197)
- Sandrelli, F., and others. 2007. A molecular basis for natural selection at the timeless locus in *Drosophila melanogaster*. Science **316**: 1898–1900. doi:[10.1126/science.1138426](https://doi.org/10.1126/science.1138426)
- Saumweber, W. J., and E. G. Durbin. 2006. Estimating potential diapause duration in *Calanus finmarchicus*. Deep-Sea Res. Part II Top. Stud. Oceanogr. **53**: 2597–2617. doi:[10.1016/j.dsr2.2006.08.003](https://doi.org/10.1016/j.dsr2.2006.08.003)
- Schlitzer, R. 2007. Ocean Data View. odv.awi.de. <https://ci.ni.ac.jp/naid/10021083844/>
- Søreide, J. E., E. Leu, J. Berge, M. Graeve, and S. Falk-Petersen. 2010. Timing of blooms, algal food quality and *Calanus glacialis* reproduction and growth in a changing Arctic. Glob. Chang. Biol. **16**: 3154–3163. doi:[10.1111/j.1365-2486.2010.02175.x](https://doi.org/10.1111/j.1365-2486.2010.02175.x)
- Speirs, D. C., W. S. C. Gurney, M. R. Heath, and S. N. Wood. 2005. Modelling the basin-scale demography of *Calanus finmarchicus* in the north-east Atlantic. Fish. Oceanogr. **14**: 333–358. doi:[10.1111/j.1365-2419.2005.00339.x](https://doi.org/10.1111/j.1365-2419.2005.00339.x)
- Strauss, J., and H. Dirksen. 2010. Circadian clocks in crustaceans: Identified neuronal and cellular systems. Front. Biosci. **15**: 1040–1074. doi:[10.2741/3661](https://doi.org/10.2741/3661)
- Sundby, S. 2000. Recruitment of Atlantic cod stocks in relation to temperature and advection of copepod populations. Sarsia **85**: 277–298. doi:[10.1080/00364827.2000.10414580](https://doi.org/10.1080/00364827.2000.10414580)
- Tande, K. S. 1982. Ecological investigations on the zooplankton community of Balsfjorden, northern Norway: Generation cycles, and variations in body weight and body content of carbon and nitrogen related to overwintering and reproduction in the copepod *Calanus finmarchicus* (Gunnerus). J. Exp. Mar. Bio. Ecol. **62**: 129–142. doi:[10.1016/0022-0981\(82\)90087-9](https://doi.org/10.1016/0022-0981(82)90087-9)
- Tarling, G. A., T. Jarvis, S. M. Emsley, and J. B. L. Matthews. 2002. Midnight sinking behaviour in *Calanus finmarchicus*: A response to satiation or krill predation? Mar. Ecol. Prog. Ser. **240**: 183–194. doi:[10.3354/meps240183](https://doi.org/10.3354/meps240183)
- Tarrant, A. M., M. F. Baumgartner, T. Verslycke, and C. L. Johnson. 2008. Differential gene expression in diapausing and active *Calanus finmarchicus* (Copepoda). Mar. Ecol. Prog. Ser. **355**: 193–207. doi:[10.3354/meps07207](https://doi.org/10.3354/meps07207)
- Tarrant, A. M., M. F. Baumgartner, B. H. Hansen, D. Altin, T. Nordtug, and A. J. Olsen. 2014. Transcriptional profiling of reproductive development, lipid storage and molting throughout the last juvenile stage of the marine copepod *Calanus finmarchicus*. Front. Zool. **11**: 91. doi:[10.1186/s12983-014-0091-8](https://doi.org/10.1186/s12983-014-0091-8)
- Tarrant, A. M., M. F. Baumgartner, N. S. J. Lysiak, D. Altin, T. R. Størseth, and B. H. Hansen. 2016. Transcriptional profiling of metabolic transitions during development and diapause preparation in the copepod *Calanus finmarchicus*. Integr. Comp. Biol. **56**: 1157–1169. doi:[10.1093/icb/icw060](https://doi.org/10.1093/icb/icw060)
- Thaben, P. F., and P. O. Westermark. 2014. Detecting rhythms in time series with RAIN. J. Biol. Rhythms **29**: 391–400. doi:[10.1177/0748730414553029](https://doi.org/10.1177/0748730414553029)
- Thurley, K., C. Herbst, F. Wesener, B. Koller, T. Wallach, B. Maier, A. Kramer, and P. O. Westermark. 2017. Principles for circadian orchestration of metabolic pathways. Proc. Natl. Acad. Sci. USA **114**: 1572–1577. doi:[10.1073/pnas.1613103114](https://doi.org/10.1073/pnas.1613103114)
- Tittensor, D. P., B. DeYoung, and C. L. Tang. 2003. Modelling the distribution, sustainability and diapause emergence timing of the copepod *Calanus finmarchicus* in the Labrador Sea. Fish. Oceanogr. **12**: 299–316. doi:[10.1046/j.1365-2419.2003.00266.x](https://doi.org/10.1046/j.1365-2419.2003.00266.x)
- van Haren, H., and T. J. Compton. 2013. Diel vertical migration in Deep Sea plankton is finely tuned to latitudinal and seasonal day length. PLoS One **8**: e64435. doi:[10.1371/journal.pone.0064435](https://doi.org/10.1371/journal.pone.0064435)
- Walkusz, W., S. Kwasniewski, S. Falk-Petersen, H. Hop, V. Tverberg, P. Wieczorek, and J. M. Weslawski. 2009. Seasonal and spatial changes in the zooplankton community of Kongsfjorden, Svalbard. Polar Res. **28**: 254–281. doi:[10.1111/j.1751-8369.2009.00107.x](https://doi.org/10.1111/j.1751-8369.2009.00107.x)
- Warnes, G. R., , and others.. 2016. Gplots: Various R programming tools for plotting data.
- Watson, N. H. F., and B. N. Smallman. 1971. The role of photoperiod and temperature in the induction and termination of an arrested development in two species of freshwater cyclopoid copepods. Can. J. Zool. **49**: 855–862. doi:[10.1139/z71-128](https://doi.org/10.1139/z71-128)
- Wilson, R. J., M. R. Heath, and D. C. Speirs. 2016. Spatial modeling of *Calanus finmarchicus* and *Calanus helgolandicus*: Parameter differences explain differences in biogeography. Front. Mar. Sci. **3**: 1–15. doi:[10.3389/fmars.2016.00157](https://doi.org/10.3389/fmars.2016.00157)
- Wood, B. J. B., P. B. Tett, and A. Edwards. 1973. An introduction to the phytoplankton, primary production and relevant hydrography of Loch Etive. J. Ecol. **61**: 569–585. doi:[10.2307/2259045](https://doi.org/10.2307/2259045)

**Acknowledgment**

We wish to thank the crew of RV *Calanus* as well as Laura Halbach (AWI) for their support during the extensive field samplings. Our work would further not have been possible without the technical support by Kerstin Oetjen and Christiane Lorenzen (AWI) as well as Chris Beveridge, John Beaton, and Colin Griffith (SAMS). Laura Hobbs, Estelle Dumont, and Finlo Cottier (SAMS) generously handled ADCP and CTD data. Our work is part of the Helmholtz Virtual Institute “PolarTime” (VH-VI-500: Biological timing in a changing marine environment—clocks and rhythms in polar pelagic organisms) funded by the Helmholtz Association of German Research Centres. Kim S. Last and David W. Pond received a small grant from SAMS (EtimeEar:1558). Bettina Meyer and Kim S. Last further received FRAM Centre incentive funding for the participation in a chronobiological workshop by Akvaplan-niva (coordinator: Eva Leu). The

work contributes to the Polar Regions and Coasts in a Changing Earth System program (PACES, Topic 1, WP 4) of the Alfred Wegener Institute Helmholtz Centre for Polar and Marine Research.

**Conflict of Interest**

None declared.

*Submitted 22 December 2017*

*Revised 28 April 2018*

*Accepted 26 June 2018*

*Associate editor: Thomas Kiørboe*

Supplemental material to:

Häfker et al. “*Calanus finmarchicus* seasonal cycle and diapause in relation to gene expression, physiology and endogenous clocks”

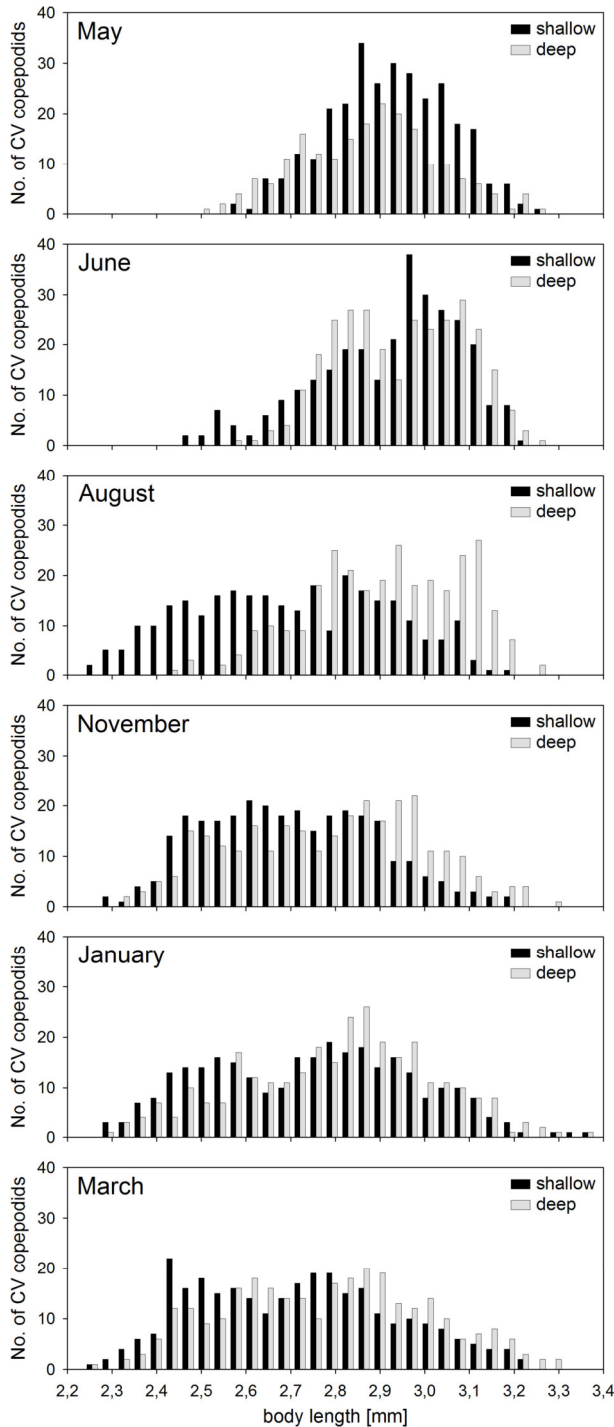


Figure S1: Seasonal change in *C. finmarchicus* CV copepodid length

distribution. For each seasonal time point and depth  $n=100$  individuals were measured. Body length was measured from the tip of the head to the end of the furca. The increase in the number of smaller sized CV copepodids in the shallow layer in August reflects the appearance of the 2<sup>nd</sup> generation occurrence of smaller sized copepods in the deep layer in November reflect the descent of the G<sub>2</sub> to diapause. The similar size distributions in both depth from November to March furthermore supports the assumption that shallow layer copepods had been advected from the deep layer.

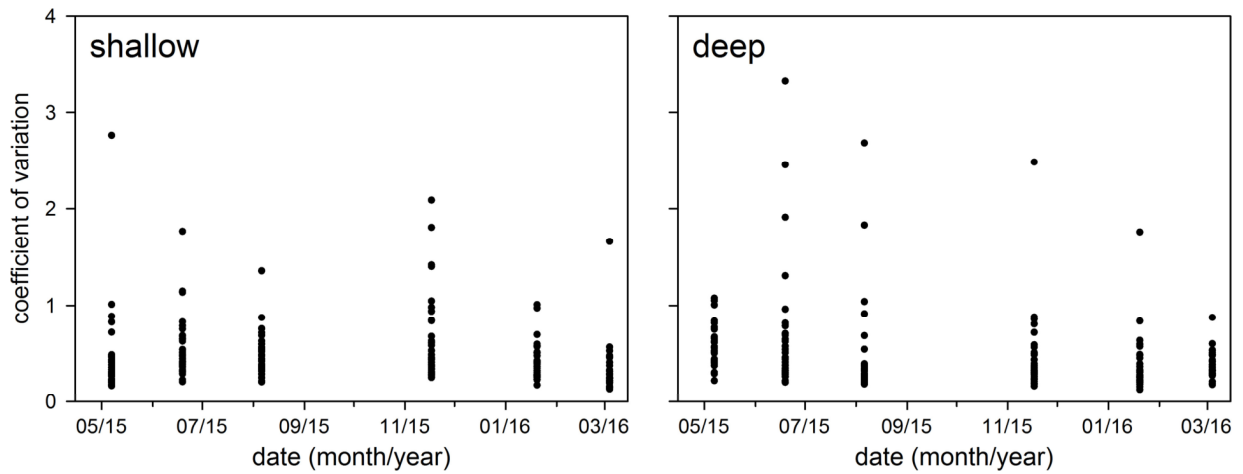


Figure S2: Seasonal change in gene expression variance. Coefficients of variation (SD divided by mean) in (A) the shallow and deep layer for all genes are shown. Date labels indicate the 1<sup>st</sup> day of the respective month. Each dot represents one gene at the respective seasonal time point. Note that while some genes show increased variation at specific seasonal time points (e.g. November/shallow, June/deep), the variance for most of the genes stayed consistently low throughout our study. This applies also to the phase of emergence in January/March 2016.

**Table S1: List of investigated genes.** Gene names, abbreviations and physiological functions are shown. Gene sequences were taken from a *C. finmarchicus* de novo transcriptome (Christie et al. 2013a, Lenz et al. 2014). All annotations were verified via blastx against NCBI database and the respective top-hit as well as the e-value and sequence identity are shown. Reference genes are listed at the bottom.

| <i>Calanus finmarchicus</i>                              |              |                     |                           | NCBI top-hit               |                           | Comparison |          |
|--|--------------|---------------------|---------------------------|----------------------------|---------------------------|------------|----------|
| gene   | abbrev.      | function            | Accession No <sup>o</sup> | species                    | Accession No <sup>o</sup> | e-value    | identity |
| <i>clock</i>   | <i>clk</i>   | clock gene          | GAXK01092177.1            | <i>T. domestica</i>        | BAJ16353.1                | 6e-152     | 61%      |
| <i>cycle</i>   | <i>cyc</i>   |                     | GAXK01131751.1            | <i>A. gambiae</i>          | XP_556301.3               | 8e-177     | 48%      |
| <i>period1</i>   | <i>per1</i>  |                     | GAXK01127710.1            | <i>M. siamensis</i>        | BAI47546.1                | 6e-96      | 32%      |
| <i>period2</i>   | <i>per2</i>  |                     | GAXK01015947.1            | <i>R. maderae</i>          | AGA01525.1                | 9e-88      | 41%      |
| <i>timeless</i>  | <i>tim</i>   |                     | GAXK01195225.1            | <i>D. erecta</i>           | XP_001968572.1            | 0.0        | 38%      |
| <i>cryptochrome2</i>                                     | <i>cry2</i>  |                     | GAXK01199676.1            | <i>S. invicta</i>          | AGD94517.1                | 0.0        | 80%      |
| <i>clockwork orange</i>                                  | <i>cwo</i>   |                     | GAXK01116566.1            | <i>L. decemlineata</i>     | AKG92774.1                | 8e-52      | 34%      |
| <i>vriille</i>   | <i>vri</i>   |                     | GAXK01130166.1            | <i>C. marinus</i>          | AFS34627.1                | 3e-44      | 61%      |
| <i>cryptochrome1</i>                                     | <i>cry1</i>  | clock light input   | GAXK01107177.1            | <i>A. mississippiensis</i> | XP_006275665.1            | 0.0        | 64%      |
| <i>doubletime2</i>                                       | <i>dbt2</i>  | clock-associated    | GAXK01058829.1            | <i>O. mykiss</i>           | CDQ75112.1                | 2e-174     | 77%      |
| <i>casein kinase II α</i>                                | <i>ck2a</i>  |                     | GAXK01065631.1            | <i>P. nana</i>             | AII16523.1                | 0.0        | 91%      |
| <i>PP2A subunit twins</i>                                | <i>tw</i>    |                     | GAXK01019902.1            | <i>S. paramamosain</i>     | AFK24473.1                | 0.0        | 89%      |
| <i>PP2A subunit widerborst</i>                           | <i>wbt1</i>  |                     | GAXK01125267.1            | <i>C. gigas</i>            | EKC28886.1                | 0.0        | 75%      |
| <i>shaggy</i>  | <i>sgg</i>   |                     | GAXK01013351.1            | <i>C. floridanus</i>       | XP_011268375.1            | 0.0        | 85%      |
| <i>phosphofructokinase</i>                               | <i>pfk</i>   | glycolysis          | GAXK01138511.1            | <i>A. aegypti</i>          | XP_001652300.1            | 0.0        | 65%      |
| <i>phosphoenolpyruvate carboxykinase</i>                 | <i>pepck</i> | gluconeogenesis     | GAXK01051558.1            | <i>H. laboriosa</i>        | KOC67158.1                | 0.0        | 60%      |
| <i>citrate synthase</i>                                  | <i>cs</i>    | citric acid cycle   | GAXK01175199.1            | <i>L. salmonis</i>         | ACO12464.1                | 0.0        | 82%      |
| <i>malate dehydrogenase</i>                              | <i>mdh</i>   |                     | GAXK01175724.1            | <i>L. salmonis</i>         | ACO12495.1                | 8e-162     | 76%      |
| <i>glutamate dehydrogenase</i>                           | <i>gdh</i>   | nitrogen metabolism | GAXK01100997.1            | <i>T. californicus</i>     | AFN54260.1                | 0.0        | 76%      |
| <i>fatty acid-binding protein</i>                        | <i>fabp</i>  | lipid anabolism     | GAXK01168773.1            | <i>C. clemensi</i>         | ACO15363.1                | 1e-32      | 49%      |
| <i>elongation of very long chain fatty acids protein</i> | <i>elov</i>  |                     | GAXK01161646.1            | <i>M. rotundata</i>        | XP_003700522.1            | 5e-79      | 51%      |
| <i>2-hydroxyacyl-CoA lyase</i>                           | <i>hacl</i>  | lipid catabolism    | GAXK01181632.1            | <i>P. xylostella</i>       | XP_011549888.1            | 0.0        | 54%      |
| <i>3-hydroxyacyl-CoA dehydrogenase</i>                   | <i>hoad</i>  |                     | GAXK01110478.1            | <i>C. gigas</i>            | XP_011451193.1            | 1e-53      | 43%      |

Table S1 (continued).

|  |                |                                |                |                        |                |        |      |
|--|----------------|--------------------------------|----------------|------------------------|----------------|--------|------|
| <i>ATP synthase <math>\gamma</math> subunit</i>    | <i>ATPsyn</i>  | respiration chain              | GAXK01169235.1 | <i>L. salmonis</i>     | ACO12344.1     | 3e-121 | 69%  |
| <i>arginine kinase</i>                             | <i>argk</i>    | anaerobic metabolism           | GAXK01169213.1 | <i>N. denticulata</i>  | BAH56608.1     | 0.0    | 83%  |
| <i>eukaryotic translation initiation factor 4E</i> | <i>if4E</i>    | translation                    | GAXK01100448.1 | <i>Z. nevadensis</i>   | KDR11192.1     | 2e-72  | 55%  |
| <i>glutathione peroxidase</i>                      | <i>gshpx</i>   | stress response                | GAXK01101248.1 | <i>L. polyphemus</i>   | XP_013772703.1 | 5e-52  | 52%  |
| <i>ferritin</i>                                    | <i>fer</i>     |                                | GAXK01170130.1 | <i>P. annandalei</i>   | AGT28487.1     | 4e-86  | 74%  |
| <i>ecdysteroid receptor</i>                        | <i>ecr</i>     | molting                        | GAXK01076616.1 | <i>C. finmarchicus</i> | ABQ57403.1     | 2e-111 | 100% |
| <i>cyclin B</i>                                    | <i>cyclB</i>   | cell cycle                     | GAXK01175362.1 | <i>C. carpio</i>       | ABX89586.1     | 1e-84  | 42%  |
| <i>couch potato</i>                                | <i>cpo</i>     | diapause-associated            | GAXK01052139.1 | <i>C. finmarchicus</i> | DAA64514.1     | 5e-117 | 99%  |
| <i>chymotrypsin</i>                                | <i>chtrp</i>   | digestion                      | GAXK01169625.1 | <i>D. pulex</i>        | EFX79589.1     | 3e-75  | 49%  |
| <i>opsin</i>                                       | <i>ops</i>     | light perception               | GAXK01018191.1 | <i>T. californicus</i> | ADZ45237.1     | 9e-158 | 62%  |
| <i>pigment-dispersing hormone receptor</i>         | <i>pdhr</i>    |                                | GAXK01203172.1 | <i>A. aegypti</i>      | XP_001653651.2 | 6e-73  | 38%  |
| <i>hemocyanin subunit</i>                          | <i>hc</i>      | blood O <sub>2</sub> transport | GAXK01053068.1 | <i>N. inaurata</i>     | CAD68057.1     | 2e-106 | 36%  |
| <i>elongation factor 1 <math>\alpha</math></i>     | <i>ef1a</i>    | reference gene                 | GAXK01169633.1 | <i>M. demolitor</i>    | XP_008547400.1 | 0.0    | 86%  |
| <i>ribosomal protein S13</i>                       | <i>rps13</i>   |                                | GAXK01165987.1 | <i>C. sinicus</i>      | ALS04988.1     | 1e-103 | 100% |
| <i>RNA polymerase II</i>                           | <i>RNApoly</i> |                                | GAXK01026612.1 | <i>C. vicinus</i>      | BAO20839.1     | 0.0    | 83%  |

1 Table S2: Changes of gene expression over the seasons and with depth. For each gene, significant  
2 differences between seasonal time points identified via Kruskal-Wallis ANOVA on Ranks are  
3 indicated by different capital letters (A,B,...) with relative expression decreasing in alphabetical  
4 order. If no letters are shown, the Kruskal-Wallis ANOVA was insignificant. The seasonal time  
5 point with maximum expression is marked with an asterisk (\*) at the respective capital letter.  
6 Significant differences between depth layers identified via Mann-Whitney U test are represented  
7 by arrows indicating higher expression in the shallow layer (↑), higher expression in the deep  
8 layer (↓) or no insignificant difference (-). max mRNA level indicates the specific maximum  
9 expression for the respective gene (minimum = 1.0). Per individual gene, month, and depth  $n=36-$   
10 40 replicates were measured. A detailed characterization of genes is given in Table S1.  
11

| gene        | depth   | Statistical analyses ( $\alpha=0.0001$ ) |          |         |          |         |         | max mRNA level |
|-------------|---------|--|----------|---------|----------|---------|---------|----------------|
|             |         | May                                      | Jun      | Aug     | Nov      | Jan     | Mar     |                |
| <i>clk</i>  | shallow | AB*                                      | AB       | BC      | A        | CD      | D       | 3.91           |
|             | deep    | ↑<br>CD                                  | -<br>AB  | ↓<br>A  | -<br>A*  | ↓<br>BC | ↓<br>D  | 3.42           |
| <i>cyc</i>  | shallow | A*                                       | A        | A       | AB       | B       | B       | 6.90           |
|             | deep    | ↑<br>A                                   | -<br>A*  | ↑<br>AB | -<br>ABC | -<br>BC | -<br>C  | 4.12           |
| <i>per1</i> | shallow | B  | B        | B       | A*       | B       | C       | 4.38           |
|             | deep    | -<br>BC                                  | ↓<br>A*  | ↓<br>A  | ↓<br>A   | ↓<br>B  | ↓<br>C  | 7.46           |
| <i>per2</i> | shallow | A*                                       | AB       | B       | AB       | C       | C       | 8.41           |
|             | deep    | -<br>A                                   | -<br>A*  | -<br>A  | -<br>A   | ↓<br>B  | ↓<br>B  | 7.22           |
| <i>tim</i>  | shallow | B  | B        | B       | A*       | B       | C       | 5.06           |
|             | deep    | -<br>C                                   | ↓<br>AB* | ↓<br>AB | ↓<br>A   | ↓<br>B  | ↓<br>C  | 9.59           |
| <i>cry2</i> | shallow | B  | B        | B       | A*       | AB      | C       | 6.98           |
|             | deep    | -<br>C                                   | ↓<br>AB  | ↓<br>AB | ↓<br>A*  | ↓<br>B  | ↓<br>C  | 13.09          |
| <i>cwo</i>  | shallow | AB                                       | AB*      | AB      | A        | BC      | C       | 3.79           |
|             | deep    | -<br>BC                                  | -<br>A*  | -<br>A  | -<br>B   | ↓<br>B  | -<br>C  | 4.10           |
| <i>vri</i>  | shallow | AB                                       | A*       | AB      | BC       | BC      | C       | 2.75           |
|             | deep    | -<br>CD                                  | ↓<br>A*  | ↓<br>AB | ↓<br>BC  | -<br>CD | -<br>D  | 5.22           |
| <i>cry1</i> | shallow | B  | AB       | AB      | B        | AB      | A*      | 1.60           |
|             | deep    | -<br>B                                   | -<br>B   | -<br>Ab | -<br>AB  | -<br>AB | -<br>A* | 1.76           |
| <i>dbt2</i> | shallow | A  | A*       | AB      | BC       | BC      | C       | 3.19           |
|             | deep    | ↑<br>B                                   | -<br>A*  | -<br>AB | -<br>B   | -<br>BC | -<br>C  | 3.81           |
| <i>ck2a</i> | shallow | A  | A        | A       | B        | A       | A*      | 1.63           |
|             | deep    | -<br>AB*                                 | ↑<br>BC  | ↑<br>C  | -<br>C   | -<br>BC | -<br>A  | 1.55           |

Table S2 (continued).

|               |         |     |    |     |     |    |    |         |
|---------------|---------|-----|----|-----|-----|----|----|---------|
| <i>tws</i>    | shallow | AB  | A* | AB  | C   | B  | A  | 4.40    |
|               | deep    | –   | ↑  | ↑   | –   | ↑  | ↑  | 3.71    |
| <i>wbt1</i>   | shallow | –   | –* | –   | –   | –  | –  | 1.12    |
|               | deep    | BCD | A* | ABC | AB  | CD | D  | 1.64    |
| <i>sgg</i>    | shallow | AB  | AB | B   | A*  | B  | C  | 2.77    |
|               | deep    | –   | ↓  | ↓   | ↓   | ↓  | ↓  | 4.16    |
| <i>pfk</i>    | shallow | CD  | A  | AB  | A*  | BC | D  | 12.94   |
|               | deep    | A*  | Ab | AB  | BC  | C  | C  | 7.51    |
| <i>pepck</i>  | shallow | ↑   | ↑  | ↑   | ↑   | –  | –  | 2.87    |
|               | deep    | A*  | AB | B   | C   | C  | C  | 4.28    |
| <i>cs</i>     | shallow | –   | –* | –   | –   | –  | –  | 1.56    |
|               | deep    | –   | –  | –   | ↓   | –  | –  | 1.59    |
| <i>mdh</i>    | shallow | B   | A* | B   | B   | C  | BC | 3.23    |
|               | deep    | A*  | A  | AB  | B   | AB | A  | 3.14    |
| <i>gdh</i>    | shallow | –   | –  | –   | –   | –  | –  | 10.78   |
|               | deep    | AB  | BC | BC  | ABC | C  | A* | 12.24   |
| <i>fabp</i>   | shallow | A   | A  | A   | B   | A  | A* | 16.44   |
|               | deep    | –   | ↑  | ↑   | –   | ↑  | –  | 9.96    |
| <i>elov</i>   | shallow | A*  | B  | B   | AB  | C  | C  | 5477.14 |
|               | deep    | ↑   | ↓  | ↓   | ↓   | ↓  | ↓  | 2692.01 |
| <i>hacl</i>   | shallow | BC  | A* | AB  | A   | C  | D  | 9.93    |
|               | deep    | A*  | A  | A   | A   | A  | B  | 7.11    |
| <i>hoad</i>   | shallow | A*  | AB | AB  | BC  | CD | D  | 4.62    |
|               | deep    | ↑   | –  | ↓   | ↓   | ↓  | ↓  | 5.39    |
| <i>ATPsyn</i> | shallow | C   | A* | AB  | A   | BC | D  | 2.11    |
|               | deep    | A*  | AB | B   | C   | B  | B  | 2.33    |
| <i>argk</i>   | shallow | –   | ↑  | ↑   | –   | ↑  | –  | 3.95    |
|               | deep    | A*  | B  | B   | B   | B  | A  | 5.80    |
| <i>if4E</i>   | shallow | BC  | C  | C   | AB* | C  | D  | 2.89    |
|               | deep    | –   | ↓  | ↓   | ↓   | ↓  | ↓  | 2.85    |
| <i>gshpx</i>  | shallow | BC  | A  | A   | A*  | AB | C  | 9.47    |
|               | deep    | AB  | D  | CD  | D   | BC | A* | 12.31   |

Table S2 (continued).

|              |         |    |    |    |    |     |    |       |
|--------------|---------|----|----|----|----|-----|----|-------|
| <i>fer</i>   | shallow | D  | BC | BC | A* | AB  | CD | 11.05 |
|              |         | ↓  | ↓  | ↓  | ↓  | ↓   | ↓  |       |
|              | deep    | C  | A* | A  | A  | B   | BC | 31.23 |
| <i>ecr</i>   | shallow | B  | AB | B  | C  | B   | A* | 4.04  |
|              |         | –  | ↑  | ↑  | –  | –   | –  |       |
|              | deep    | AB | C  | C  | BC | BC  | A* | 3.57  |
| <i>cyclB</i> | shallow | B  | B  | B  | C  | AB  | A* | 20.11 |
|              |         | –  | ↑  | ↑  | –  | ↑   | –  |       |
|              | deep    | AB | C  | C  | C  | B   | A* | 17.45 |
| <i>cpo</i>   | shallow | B  | B  | AB | A* | B   | C  | 3.34  |
|              |         | –  | ↓  | ↓  | –  | ↓   | ↓  |       |
|              | deep    | CD | AB | A  | A* | BC  | D  | 4.25  |
| <i>chtrp</i> | shallow | A* | AB | B  | B  | C   | C  | 68.08 |
|              |         | –  | ↑  | ↑  | ↑  | ↑   | ↑  |       |
|              | deep    | A* | CD | BC | D  | BCD | AB | 47.92 |
| <i>ops</i>   | shallow | C  | C  | BC | A* | AB  | D  | 5.21  |
|              |         | –  | ↓  | ↓  | –  | ↓   | ↓  |       |
|              | deep    | B  | A  | A  | A* | A   | B  | 8.81  |
| <i>pdhr</i>  | shallow | A  | A  | A  | A* | B   | B  | 4.12  |
|              |         | –  | ↓  | ↓  | –  | –   | ↑  |       |
|              | deep    | BC | A* | AB | B  | CD  | D  | 6.88  |
| <i>hc</i>    | shallow | D  | BC | BC | A* | AB  | CD | 21.81 |
|              |         | ↓  | ↓  | ↓  | –  | ↓   | ↓  |       |
|              | deep    | B  | A  | A  | A* | A   | B  | 24.41 |